UNCLASSIFIED

SC 1004-A (3-55)

[redacted]

[redacted]

[redacted]

SANDIA SYSTEMATIC DECLASSIFICATION REVIEW	
1st Review Date: 6-1-79	Determination (Circle Numbers):
Authority: ☐ADC ☒ADD	1. Classification Retained
Name: CCRP-RB	2. Classification Changed to: U
2nd Review Date: 10-21-96	3. Contains No DOE Classified Information
Authority: ADD	4. Coordinate With:
Name: W. Layne	5. Contains UCAI?
	6. Comments: Unclassified

SCTM-168-57-51

SCTM-168-57-51

RESULTS OF WIND-TUNNEL TESTS OF THE SECOND SERIES OF AERODYNAMIC SHAPES PROPOSED FOR USE AS A SHORT 7 WEAPON

SANDIA SYSTEMATIC DECLASSIFICATION REVIEW DOWNGRADING OR DECLASSIFICATION STAMP	
CLASSIFICATION CHANGED TO: U	AUTHORITY: W. C. Layne
Emelda Selph 10-23-96	RECORD ID: 97SN039
PERSON CHANGING MARKING & DATE: R.T. Duff 10/29/96	DATED: 10-21-96
PERSON VERIFYING MARKING & DATE	

S. S. Millwright - 5142
R. L. Black - 5142

ABSTRACT

Stability coefficients obtained from tests conducted at the Sandia Corporation 3-inch open-jet wind tunnel are presented and compared with stability coefficients obtained from tests conducted at three larger wind tunnels. A satisfactory aerodynamic shape is recommended.

Work performed under AEC Contract AT-(29-1)-789.

[redacted]

Case No. 409.01

June 25, 1957

UNCLASSIFIED

[redacted]

DISTRIBUTION:
S. C. Hight, 5100
A. Y. Pope, 5140
P. W. Rowe, 5141
R. C. Maydew, 5142
K. F. Crowder, 5143
W. H. Curry, 5144
J. McMinn, 1832-3
R. K. Smeltzer, 7221-3
L. F. Parman, 7223 (6)

TABLE OF CONTENTS

	Page
SUMMARY	6
INTRODUCTION	7
AERODYNAMIC SYMBOLS	7
DISCUSSION	8
General	8
SCARF II Test Program Results	9
Comparison of SCARF II Data with CWT, CAL, and IAL Data	10
Recommended Shape	10
CONCLUSIONS	10
LIST OF REFERENCES	11
APPENDIX A -- CONFIGURATION NOMENCLATURE	12
APPENDIX B -- CONFIGURATIONS TESTED	13

LIST OF ILLUSTRATIONS

		Page
Fig. 1a	-- Basic body shapes with Mk 5 type noses	17
Fig. 1b	-- Basic body shapes	18
Fig. 2	-- Basic fin shapes.	19
Fig. 3	-- Basic nose shapes	20
Fig. 4a	-- C_{m_α} vs Mach number (Mod 1).	21
Fig. 4b	-- $(C_{m_q} + C_{m_{\dot\alpha}})$ vs Mach number (Mod 1).	22
Fig. 5a	-- C_{m_α} vs Mach number (Mod 2).	23
Fig. 5b	-- $(C_{m_q} + C_{m_{\dot\alpha}})$ vs Mach number (Mod 2).	24
Fig. 6a	-- C_{m_α} vs Mach number (Mod 3).	25
Fig. 6b	-- $(C_{m_q} + C_{m_{\dot\alpha}})$ vs Mach number (Mod 3).	26
Fig. 7a	-- C_{m_α} vs Mach number (Mod 4).	27
Fig. 7b	-- $(C_{m_q} + C_{m_{\dot\alpha}})$ vs Mach number (Mod 4).	28
Fig. 8a	-- C_{m_α} vs Mach number (Mod 5).	29
Fig. 8b	-- C_{m_α} vs Mach number (Mod 5).	30
Fig. 8c	-- $(C_{m_q} + C_{m_{\dot\alpha}})$ vs Mach number (Mod 5).	31
Fig. 8d	-- $(C_{m_q} + C_{m_{\dot\alpha}})$ vs Mach number (Mod 5).	32
Fig. 9a	-- C_{m_α} vs Mach number (Mod 6).	33

LIST OF ILLUSTRATIONS (Cont)

Page

Fig. 9b -- $(C_{m_q} + C_{m_{\dot{\alpha}}})$ vs Mach number (Mod 6) 34

Fig. 10a -- C_{m_α} vs Mach number (Mod 7) 35

Fig. 10b -- $(C_{m_q} + C_{m_{\dot{\alpha}}})$ vs Mach number (Mod 7) 36

Fig. 11a -- C_{m_α} vs Mach number (Mod 8) 37

Fig. 11b -- $(C_{m_q} + C_{m_{\dot{\alpha}}})$ vs Mach number (Mod 8) 38

Fig. 12a -- Comparison of the static stability coefficients obtained in CWT and SCARF II on models of the Short 7 Mod 4. 39

Fig. 12b -- Comparison of the dynamic stability coefficients obtained in CWT and SCARF II on models of the Short 7 Mod 4. 40

Fig. 13 -- Comparison of C_{m_α} obtained in CAL and SCARF II on models of the Short 7 Mod 8 41

Fig. 14a -- Comparison of C_{m_α} obtained in LAL, CAL, and SCARF II on models of the Short 7. 42

Fig. 14b -- Comparison of $(C_{m_q} + C_{m_{\dot{\alpha}}})$ obtained in LAL, CAL, and SCARF II on models of the Short 7. 43

Fig. 15a -- Static stability characteristics of the TX-14 (CARRIE) with different fin configurations 44

Fig. 15b -- Dynamic stability characteristics of the TX-14 (CARRIE) with different fin configurations 45

Fig. 16 -- Retractable fin TX-14 (CARRIE) shape 46

SUMMARY

Eight basic body shapes (proposed for the Short 7 ballistic case) with various fin and spoiler-band configurations were tested in the Sandia Corporation 3-inch open-jet wind tunnel. The stability data obtained indicated that three of the shapes showed sufficient promise to warrant additional investigation. Stability data obtained with the 3-inch jet agree qualitatively with data obtained at CAL, CWT, and LAL. The wind-tunnel data indicate the TX-14 (CARRIE) shape with the retractable fin configuration exhibits satisfactory stability characteristics.

RESULTS OF WIND-TUNNEL TESTS OF THE SECOND SERIES OF AERODYNAMIC SHAPES PROPOSED FOR USE AS A SHORT 7 WEAPON

INTRODUCTION

In July 1954 it was learned that the proposed shape for the Short 7 weapon was not aerodynamically satisfactory. A completely new study[1] was then proposed with several basic body shapes considered.

The models were fabricated for testing in the Sandia Corporation Aerodynamic Research Facility (hereinafter called SCARF II).[2] The first run was made on August 31, 1954. From the SCARF II data it was determined that only three of these models showed sufficient promise to warrant further investigation.

Two of these models were tested at Cooperative Wind Tunnel (CWT);[3] the third was tested at Cornell Aeronautical Laboratory (CAL).[4] In addition to these three models, a more reliable "fix" was sought by the adaption of retractable-type fins on the basic TX-14 (CARRIE) shape. The TX-14 shape was tested at a larger wind tunnel (CWT) only.

The purpose of this memorandum is to present the stability data obtained from SCARF II, compare these data with data obtained from three larger wind tunnels, and to recommend a satisfactory aerodynamic shape.

AERODYNAMIC SYMBOLS

C_m Pitching moment coefficient $= \frac{\bar{M}}{\bar{q}Sd}$

C_{m_α} Rate of change of pitching moment coefficient with angle of attack, $\frac{\partial C_m}{\partial \alpha}$, per degree

C_{m_q} Rate of change of pitching moment coefficient with pitching velocity, $\frac{\partial C_m}{\partial \frac{qd}{2V}}$, per radian

$C_{m_{\dot{\alpha}}}$ Rate of change of pitching moment coefficient with rate of change of angle of attack, $\frac{\partial C_m}{\partial \frac{\dot{\alpha}d}{2V}}$, per radian

d	Maximum diameter of model, ft
$\overline{M}$	Model pitching moment about store center of gravity, ft-lb
P_a	Ambient or free-stream pressure, lb/ft^2
q	Pitching velocity, rad/sec
$\overline{q}$	Dynamic pressure $= \frac{1}{2}\rho V^2 = \frac{\gamma}{2} P_a M^2$, lb/ft^2
S	Store frontal area $= \frac{\pi d^2}{4}$, ft^2
t	Time, seconds
V	Velocity, ft/sec
α	Angle of attack, degrees
$\dot{\alpha}$	Rate of change of angle of attack, $\frac{\partial \alpha}{\partial t}$, rad/sec
γ	Ratio of specific heats, taken as 1.4 for air
ρ	Density of free-stream air, $slugs/ft^3$

DISCUSSION

General

The obstacle which presented the greatest challenge in developing an aerodynamically stable Short 7 was the stipulation, predicated on aircraft compatability, that the fins could not extend beyond the maximum diameter of the body. In the event that no satisfactory ballistic shape could be found with this restriction, a more positive "fix" was sought through the use of retractable-type fins on the TX-14 (CARRIE) shape. This type fin would be least desirable from an engineering standpoint because of the added complexity.

Eight basic body shapes (Figs. 1a and 1b) were tested at SCARF II. Various fins (Fig. 2), noses (Fig. 3), and spoiler bands were tried on these basic shapes in an effort to find a stable configuration. Refer to Appendices A and B for model nomenclature and run list.

Of the eight shapes tested at SCARF II, only three shapes were considered promising enough to warrant further investigation at larger wind tunnels.

SCARF II Test Program Results

Mod 1 stability curves (Figs. 4a and 4b) show two configurations statically unstable, three configurations statically stable, and all configurations dynamically stable through the Mach number range. The configuration tested in run No. 16 had such a high degree of static instability that the data were not plotted in Figs. 4a or 4b. (Such statically unstable configurations occurred throughout the SCARF II program. These configurations are tabulated on plots according to their respective "Mod numbers", but the data are not plotted.)

Mod 2 was one of the basic body shapes selected to be tested in the larger tunnels. Figure 5a shows that two of the Mod 2 configurations were statically stable and two were statically unstable or showed marginal static stability.

Figure 5b shows that four of the Mod 2 configurations tested possessed good dynamic stability in the lower and intermediate Mach number range. These four configurations showed decreasing dynamic stability near the upper end of the Mach number range.

Figures 6a and 6b reveal that two configurations of Mod 3 became statically unstable near the upper portion of the Mach number range. These same two configurations were dynamically stable throughout the Mach number range.

Mod 4 was the second of the three shapes chosen to be tested in the larger tunnels. Static stability curves (Fig. 7a) for three configurations of Mod 4 indicate stability up to M = 0.83 for one configuration while two configurations had marginal static stability.

These three Mod 4 configurations were dynamically stable throughout the Mach number range (Fig. 7b).

Three configurations of Mod 5 possessed static stability as shown in Figs. 8a and 8b. All nine configurations of Mod 5 had good dynamic stability characteristics (Figs. 8c and 8d).

The Mod 5 stability data from SCARF II seem to indicate that this body shape should have been chosen as one of the shapes to be further investigated at a larger tunnel. However, it was discovered that the volume of this shape was insufficient to contain the necessary weapon components.

Two configurations of Mod 6 were statically stable up to M = 0.90 (Fig. 9a). These same Mod 6 configurations were dynamically stable throughout the Mach number range (Fig. 9b).

The data from one Mod 7 configuration plotted in Figs. 10a and 10b shows this configuration to be both statically and dynamically stable.

Mod 8 static stability data (Fig. 11a) show the model unstable above M = 0.62. Mod 8 dynamic stability data (Fig. 11b) indicate the model is stable throughout the Mach number range. Mod 8 was the third model chosen to be tested at a larger tunnel.

Comparison of SCARF II Data with CAL, CWT, and LAL Data

The trend of SCARF II static stability data for Mod 4 (Fig. 12a) compares favorably with the trend of static stability data for Mod 4 as obtained from CWT (Fig. 12a). However, the magnitudes of the static stability coefficients from the two tunnels vary greatly throughout the Mach number range.

Dynamic stability curves for Mod 4 (Fig. 12b) compare well up to M = 0.86. Above M = 0.86 CWT data show the model becoming dynamically unstable, while the SCARF II data indicate that the model remains dynamically stable through the upper end of the Mach number range.

Figure 13 shows that SCARF II static stability data for Mod 8 follow the static stability data from CAL closely up to M = 0.8. Above M = 0.8 SCARF II data disagree with CAL data as to the degree of static instability.

Static and dynamic stability data on the original Short 7 shape are contained in Figs. 14a and 14b. Static stability data from CAL agree with static stability data from LAL. Both of these tests show the model remaining statically stable throughout the Mach number range, but additional tests (data which are not contained in this report) indicate static instability above M = 0.95. SCARF II data for the same configuration show the model becoming statically unstable at M = 0.86.

Dynamic stability data from SCARF II, CAL, and LAL (Fig. 14b) agree closely and indicate this configuration is stable throughout the Mach number range.

Recommended Shape

Static stability data for the TX-14 (CARRIE) shape (Fig. 15a) show the retractable fin configurations (Runs 24 and 31) are more stable than the fixed-fin configurations. These retractable fin configurations are also dynamically more stable than the fixed-fin configurations (Fig. 15b).

CONCLUSIONS

1. None of the new Short 7 configurations are aerodynamically acceptable if the engineering standards dictating fin span, etc., are met.
2. The shape that is most desirable from an aerodynamic viewpoint is that of the TX-14 (CARRIE) body, nose, and spoiler bands with retractable-type fins (see Fig. 16) (CWT Run 24, Figs. 15a and 15b).

S. S. MILLWRIGHT - 5142
R. L. BLACK - 5142

Case No. 409.01
June 25, 1957

LIST OF REFERENCES

1. Memorandum, Brodsky, R. F., 5141, to Hansche, G. E., 5140, Proposed Program for Short 7 Aerodynamic Studies, Ref. Sym: 5141 (526), July 29, 1954.

2. Luchter, Stephen, 5142, Performance of the Sandia 3-Inch Open-Jet Wind Tunnel, Sandia Corporation Technical Memorandum 89-54-51, May 24, 1954. *

3. Southern California Cooperative Wind Tunnel, Report on High-Speed Dynamic Wind-Tunnel Tests of the Sandia Corporation "SHRIMP", "CARRIE", "Model No. 2" and "Model No. 4" Shapes, October 6, 1955.

4. Cornell Aeronautical Laboratory Report, 846-005-1, Transonic Wind-Tunnel Tests of the Sandia Shorty Force Models, March 1955.

*Since this TM has been issued, the facility has been removed to Area 1 and now utilizes a completely different air storage source.

[redacted]

UNCLASSIFIED

APPENDIX A

CONFIGURATION NOMENCLATURE

xN_y^z	Nose section; x is model maximum diameter in inches; y is nose type (y = 54 indicates Mark V nose, y = C indicates CARRIE nose, y = T indicates 1/3 ogive nose); z is the nose length to diameter (x) ratio.
E^z	Cylindrical midsection; z is the extension length to diameter ratio.
B_y^z	Afterbody section; y is body type (y = C indicates Mod 3 body, y = 40 indicates Short 7 body) or model number; z is the body length to diameter ratio.
G^z	Center of gravity or rotation; z is center of gravity position in per cent of model length.
(P - Q)	Model stations in decimal fractions of model length where afterbody taper begins (P) and ends (Q) (Mod 5 only).
NF_{xy}^{zm}	Fins; N is number of fins, for N = 6, six fins, when N does not appear, 4 fins are indicated; x is the type of fin, i.e., WF (wedge flat), DW (double wedge) or the wedge angles in degrees, i.e., 5-25 (5° - 25° double wedge), 82-0 (82° - 0° wedge flat); y is additional information, i.e., L(long), T(thick), R(retractable), S(short); Z is the tip-to-tip span of diametrically opposed fins in terms of model maximum diameter; M indicates the fin tip is raked, modified, etc.
S_{xyza}	Spoiler bands - complete circumferential rings; x, y, and z indicate, respectively, the number of bands on the nose section, cylindrical midsection, and afterbody section.

[redacted]

APPENDIX B

CONFIGURATIONS TESTED

Facility	Run No.	Configuration	Basic body shape	Remarks
Scarf 2-3	1	$.5N_T^{1.15}E^{.4}B_2^{1.72}G^{38.2}6F_{WF}^{1.0}$	Mod 2	
Scarf 2-3	2	$.5N_T^{1.15}E^{.4}B_2^{1.72}G^{38.2}F_{WF}^{1.0}$	Mod 2	
Scarf 2-3	3	$.5N_{54}^{1.05}E^{.4}B_4^{1.47}G^{39.2}F_{WFL}^{1.08}$	Mod 4	
Scarf 2-3	4	$.5N_{54}^{1.05}E^{.4}B_4^{1.47}G^{39.2}F_{DW}^{1.08}$	Mod 4	
Scarf 2-3	5	$.5N_{54}^{1.05}E^{.4}B_4^{1.47}G^{39.2}F_{DW}^{1.0}$	Mod 4	
Scarf 2-3	6	$.5N_c^{1.13}E^{.4}B_c^{1.97}G^{35.1}F_{6-14}^{1.0}S_{302A}$	Mod 3	
Scarf 2-3	7	$.5N_{54}^{1.05}E^{.4}B_4^{1.47}G^{39.2}F_{WFS}^{1.08}$	Mod 4	
Scarf 2-3	8	$.5N_{54}^{1.05}E^{.4}B_4^{1.47}G^{39.2}F_{DW}^{1.0}S_{200B}$	Mod 4	
Scarf 2-3	9	$.5N_{54}^{1.05}E^{.4}B_1^{3.01}G^{25.2}F_{WF}^{.80M}$	Mod 1	
Scarf 2-3	10	$.5N_T^{.89}E^{.4}B_2^{1.67}G^{33.3}F_{WFT}^{1.0}$	Mod 2	
Scarf 2-3	11	$.5N_T^{.89}E^{.4}B_2^{1.67}G^{33.3}F_{DW}^{1.0}$	Mod 2	
Scarf 2-3	12	$.5N_{54}^{1.01}E^{.4}B_1^{3.01}G^{25.2}F_{WF}^{.80M}S_{200C}$	Mod 1	
Scarf 2-3	13	$.5N_T^{1.11}E^{.4}B_1^{2.91}G^{27.4}F_{WF}^{.80M}$	Mod 1	

Facility	Run No.	Configuration	Basic body shape	Remarks
Scarf 2-3	14	$.5N_T^{1.11}{}_E.{}^4B_1^{3.01}{}_G25.2_{F_{WF}}^{.80M}S_{002D}$	Mod 1	
Scarf 2-3	15	$.5N_{54}^{1.01}{}_E.{}^4B_1^{3.01}{}_G25.2_{F_{WF}}^{.80M}S_{212E}$	Mod 1	
Scarf 2-3	16	$.5N_{54}^{1.01}{}_E.{}^4B_1^{3.01}{}_G25.2_{F_{WF}}^{.80M}S_{202F}$	Mod 1	
Scarf 2-3	17	$.5N_T^{.89}{}_E.{}^4B_2^{1.67}{}_G33.3_{F_{DW}}^{1.0}S_{103G}$	Mod 2	
Scarf 2-3	18	$.5N_T^{.89}{}_E.{}^4B_2^{1.67}{}_G33.3_{F_{WFT}}^{1.0}S_{103G}$	Mod 2	
Scarf 2-3	19	$.5N_T^{.89}{}_E.{}^4B_2^{1.67}{}_G33.3_{F_{WFT}}^{1.0}S_{003H}$	Mod 2	
Scarf 2-3	20	$.5N_T^{.89}{}_E.{}^4B_2^{1.67}{}_G33.3_{F_{WFT}}^{1.0}S_{002I}$	Mod 2	
Scarf 2-3	21	$.5N_{54}^{.67}{}_E.{}^4B_{40}^{1.47}{}_G39.3_{F_{5-25}}^{1.076}S_{1130}$	Short 7	
Scarf 2-3	22	$.5N_c^{.83}{}_E.{}^4B_c^{1.70}{}_G34.9_{F_{6-14}}^{1.0}$	Mod 3	
Scarf 2-3	23	$.5N_c^{.83}{}_E.{}^4B_c^{1.70}{}_G34.9_{F_{6-14}}^{1.0}S_{302J}$	Mod 3	
Scarf 2-3	24	$.5N_{54}^{1.01}{}_E.{}^4B_6^{2.94}{}_G25.6_{F_{WF}}^{1.0M}$	Mod 6	
Scarf 2-3	25	$.5N_{54}^{1.01}{}_E.{}^4B_5^{2.94}{}_G25.6_{F_{WF}}^{1.0M}$	Mod 5	
Scarf 2-3	26	$.5N_{54}^{1.01}{}_E.{}^4B_6^{2.94}{}_G25.6_{F_{DW}}^{1.0M}S_{200C}$	Mod 6	
Scarf 2-3	27	$.5N_{54}^{1.01}{}_E.{}^4B_5^{2.94}{}_G25.6_{F_{DW}}^{1.0M}S_{200C}$	Mod 5	
Scarf 2-3	28	$.5N_{54}^{1.01}{}_E.{}^4B_7^{2.94}{}_G25.6_{F_{DW}}^{1.0M}S_{200C}$	Mod 7	
Scarf 2-3	29	$.5N_{54}^{1.01}{}_E.{}^4B_7^{2.94}{}_G25.6_{F_{WF}}^{1.0M}S_{200C}$	Mod 7	

Facility	Run No.	Configuration	Basic body shape	Remarks
Scarf 2-3	30	$.5N_{54}^{1.01}E^{.4}B_{7}^{2.94}G^{25.6}F_{WF}^{1.0M}$	Mod 7	
Scarf 2-3	31	$.5N_{54}^{1.01}E^{.4}B_{7}^{2.94}G^{25.6}F_{DW}^{1.0M}$	Mod 7	
Scarf 2-3	32	$.5N_{54}^{1.01}E^{.4}B_{5}^{2.94}G^{25.6}F_{DW}^{1.0M}$	Mod 5	
Scarf 2-3	33	$.5N_{54}^{1.01}E^{.4}B_{6}^{2.94}G^{25.6}F_{DW}^{1.0M}$	Mod 6	AL nose
Scarf 2-3	34	$.5N_{54}^{1.01}E^{.4}B_{6}^{2.94}G^{25.6}F_{DW}^{1.0M}$	Mod 6	Brass nose
Scarf 2-3	35	$.5N_{T}^{1.11}E^{.4}B_{5}^{2.94}G^{25.6}F_{DW}^{1.0M}$	Mod 5	
Scarf 2-3	36	$.5N_{54}^{1.01}E^{.4}B_{5}^{2.94}G^{25.6}F_{DW}^{1.0M}$	Mod 5	(.34-.45)
Scarf 2-3	37	$.5N_{54}^{1.01}E^{.4}B_{5}^{2.94}G^{25.6}F_{DW}^{1.0M}$	Mod 5	(.64-.64)
Scarf 2-3	38	$.5N_{54}^{1.01}E^{.4}B_{5}^{2.94}G^{25.6}F_{DW}^{1.0M}$	Mod 5	(.53-.64)
Scarf 2-3	39	$.5N_{54}^{1.01}E^{.4}B_{5}^{2.94}G^{25.6}F_{DW}^{1.0M}$	Mod 5	(.53-.53)
Scarf 2-3	40	$.5N_{54}^{1.01}E^{.4}B_{5}^{2.94}G^{25.6}F_{DW}^{1.0M}$	Mod 5	(.45-.53)
Scarf 2-3	41	$.5N_{54}^{1.01}E^{.4}B_{5}^{2.94}G^{25.6}F_{DW}^{1.0M}$	Mod 5	(.45-.45)
Scarf 2-3	42	$.5N_{54}^{1.01}E^{.4}B_{5}^{2.94}G^{25.6}F_{DW}^{1.0M}$	Mod 5	(.41-.45)
Scarf 2-3	43	$.5N_{54}^{1.01}E^{.4}B_{5A}^{2.58}G^{27.9}F_{DW}^{.98}S_{20A}$	Mod 8	
CWT 460	2	$3.5N_{54}^{.67}B_{4}^{2.25}G^{35}F_{5-25}^{1.0}S_{200A}$	Mod 4	

Facility	Run No.	Configuration	Basic body shape	Remarks
CWT 460	22	$3.5N_{T}^{.67}B_{2}^{2.28}G^{35}F_{5-25}^{1.0}$	Mod 2	
CWT 460	24	$3.0N_{c}^{.91}B_{c}^{2.69}G^{37}F_{(82-0)}^{1.52M}R^{S}_{302A}$	CARRIE	Retractable fins
WADC 126	2	$3.0N_{c}^{.91}B_{c}^{2.69}G^{37}F_{(82-0)}^{1.52M}R^{S}_{302A}$	CARRIE	Retractable fins
WADC 126	3	$3.0N_{c}^{.91}B_{c}^{2.69}G^{42}F_{(82-0)}^{1.52M}R^{S}_{302A}$	CARRIE	Retractable fins
WADC 126	4	$3.0N_{c}^{.91}B_{c}^{2.69}G^{32}F_{(82-0)}^{1.52M}R^{S}_{302A}$	CARRIE	Retractable fins
CAL 846-005*	3-21	$3.5N_{54}^{.67}B_{5A}^{3.33}F_{5-25}^{.98}S_{20A}$	Mod 8	

*Data from strain-gage balance - no dynamic stability obtained.

UNCLASSIFIED

	[redacted]	REPORT NO.
		MODEL NO.

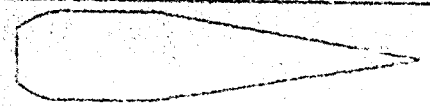

MOD 1 WITH MK 5 TYPE NOSE

L/D=4.4

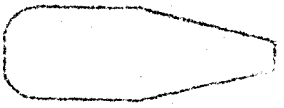

MOD 2 WITH MK 5 RAD TYPE NOSE

L/D=3

MOD 3 WITH MK 5 TYPE NOSE

L/D=[illegible]

MOD 4 WITH MK 5 TYPE NOSE

L/D=[illegible]

UNCLASSIFIED

[redacted]

FIGURE 19
BASIC BODY SHAPES

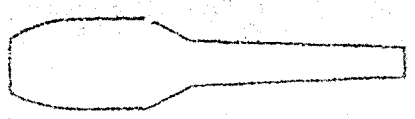

MOD 5

L/D = 4.4

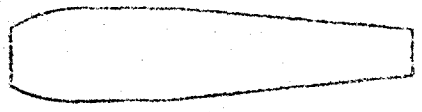

MOD 6

L/D = 4.4

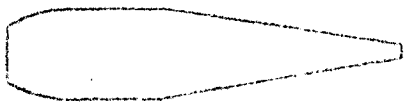

MOD 7

L/D = 4.4

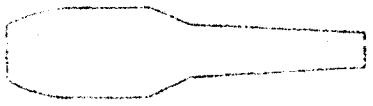

MOD 7 (SA)

L/D = 4

UNCLASSIFIED

[redacted]

FIGURE 16
BASIC BODY SHAPES
WITH
MK 5 TYPE NOSES

PREPARED BY:	SANDIA [redacted]	REPORT NO.
CHECKED BY:		
DATE:		MODEL NO.

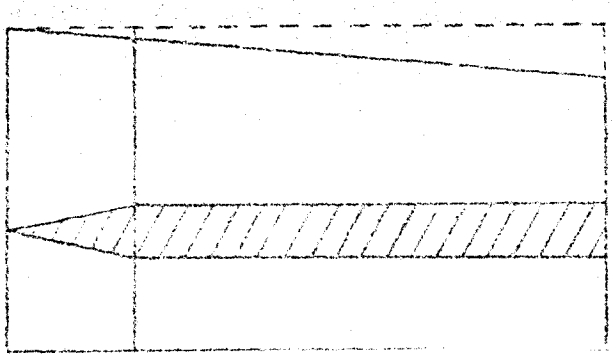

WEDGE-FLAT TYPE (WF)

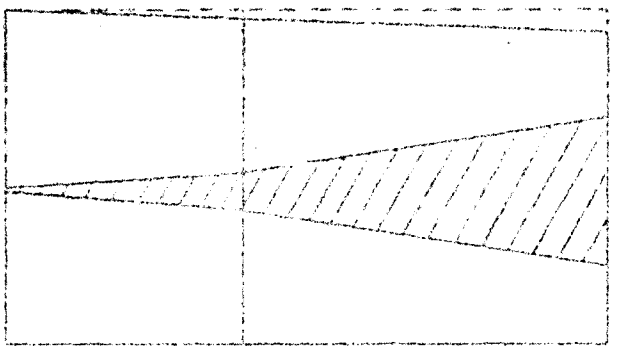

DOUBLE-WEDGE TYPE (DW)

[redacted]

FIGURE 2
BASIC FIN SHAPES

SKETCH SHEET

PREPARED BY:	SANDIA CORPORATION [redacted]	PAGE NO.
CHECKED BY:		REPORT NO.
DATE:		MODEL NO.

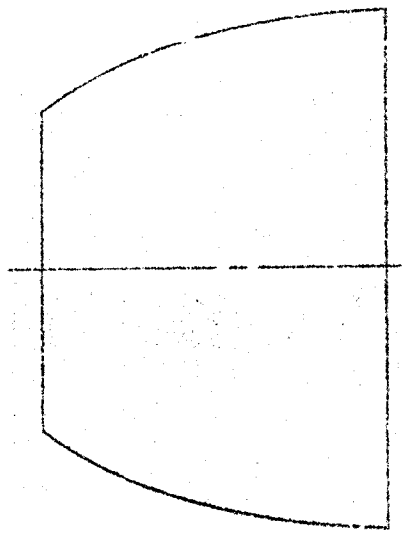

N_{S4}

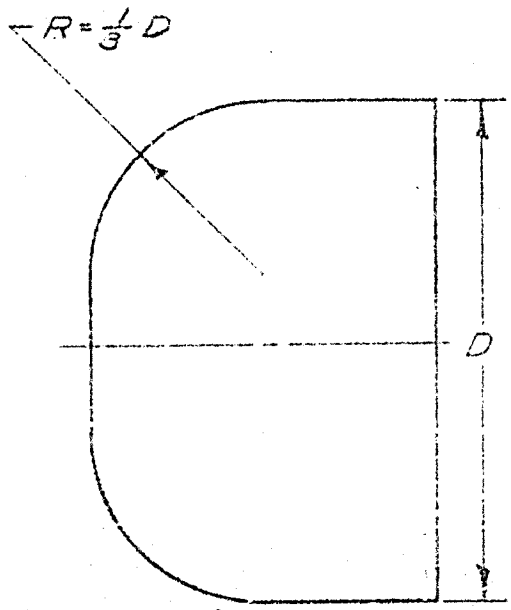

N_T

UNCLASSIFIED

[redacted]

FIGURE 3, BASIC NOSE SHAPES

UNCLASSIFIED

[redacted]

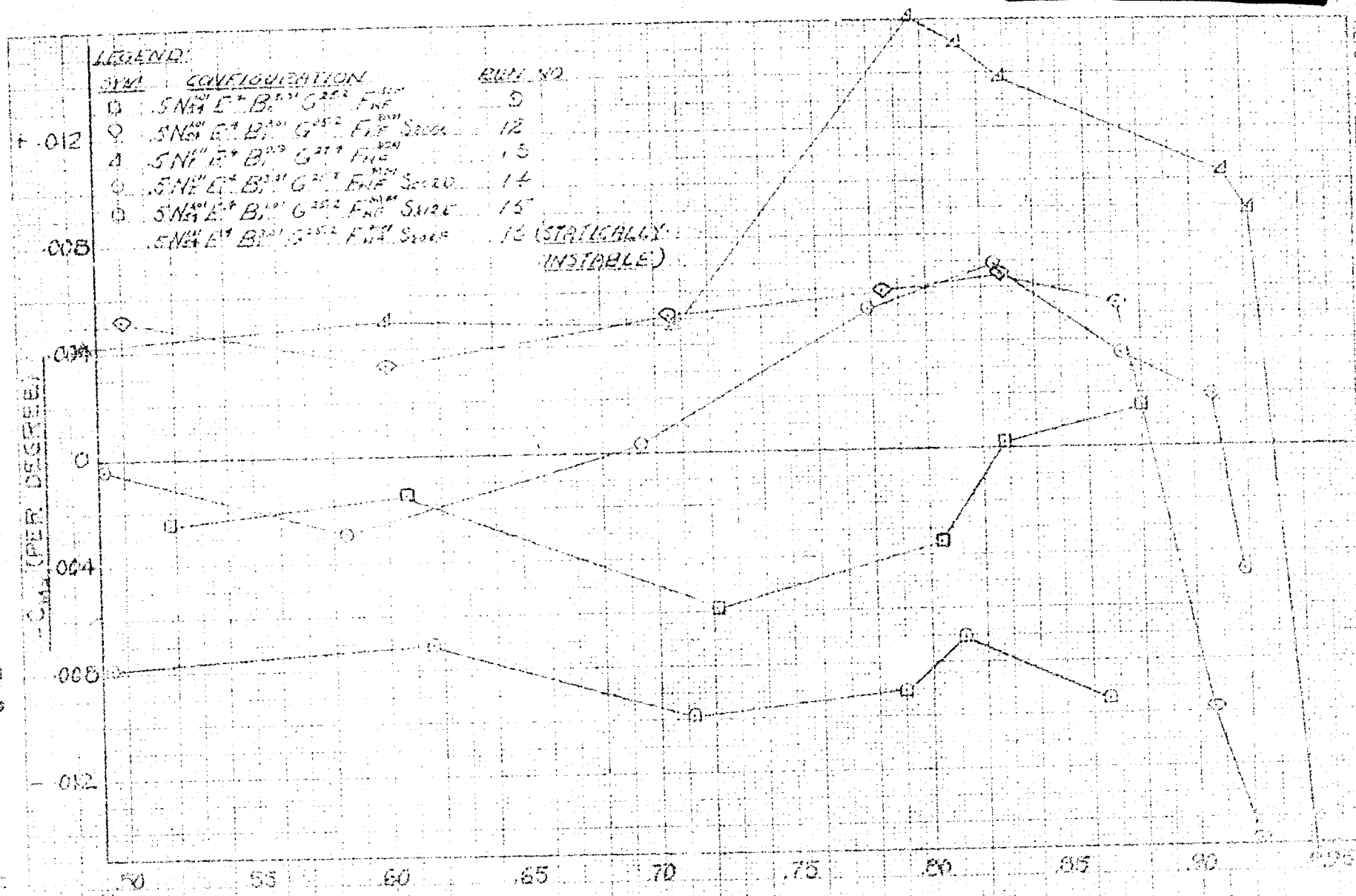

FIGURE 4A, C_{M_α} VS MACH NUMBER (MOD I)

PREP. BY RLB

UNCLASSIFIED

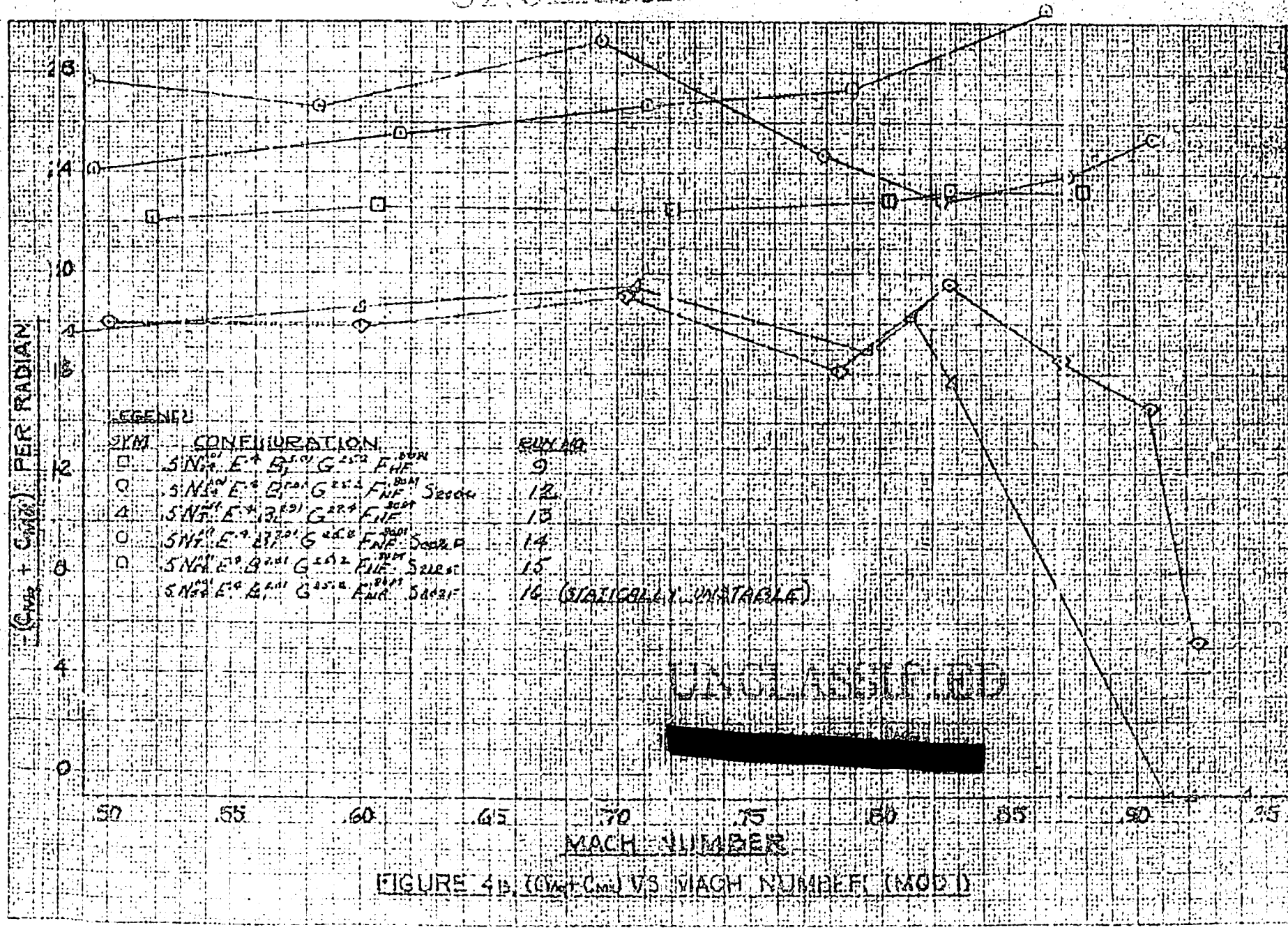

UNCLASSIFIED

[redacted]

FIGURE 4b. $(C_{m_\alpha} + C_{m_{\dot\alpha}})$ VS MACH NUMBER (MOD I)

PREP BY RLB DATE 11 SEPT '54

SANDIA CORPORATION
ALBUQUERQUE, NEW MEXICO
REPORT NO. SCARF 2-3
PAGE

UNCLASSIFIED

[redacted]

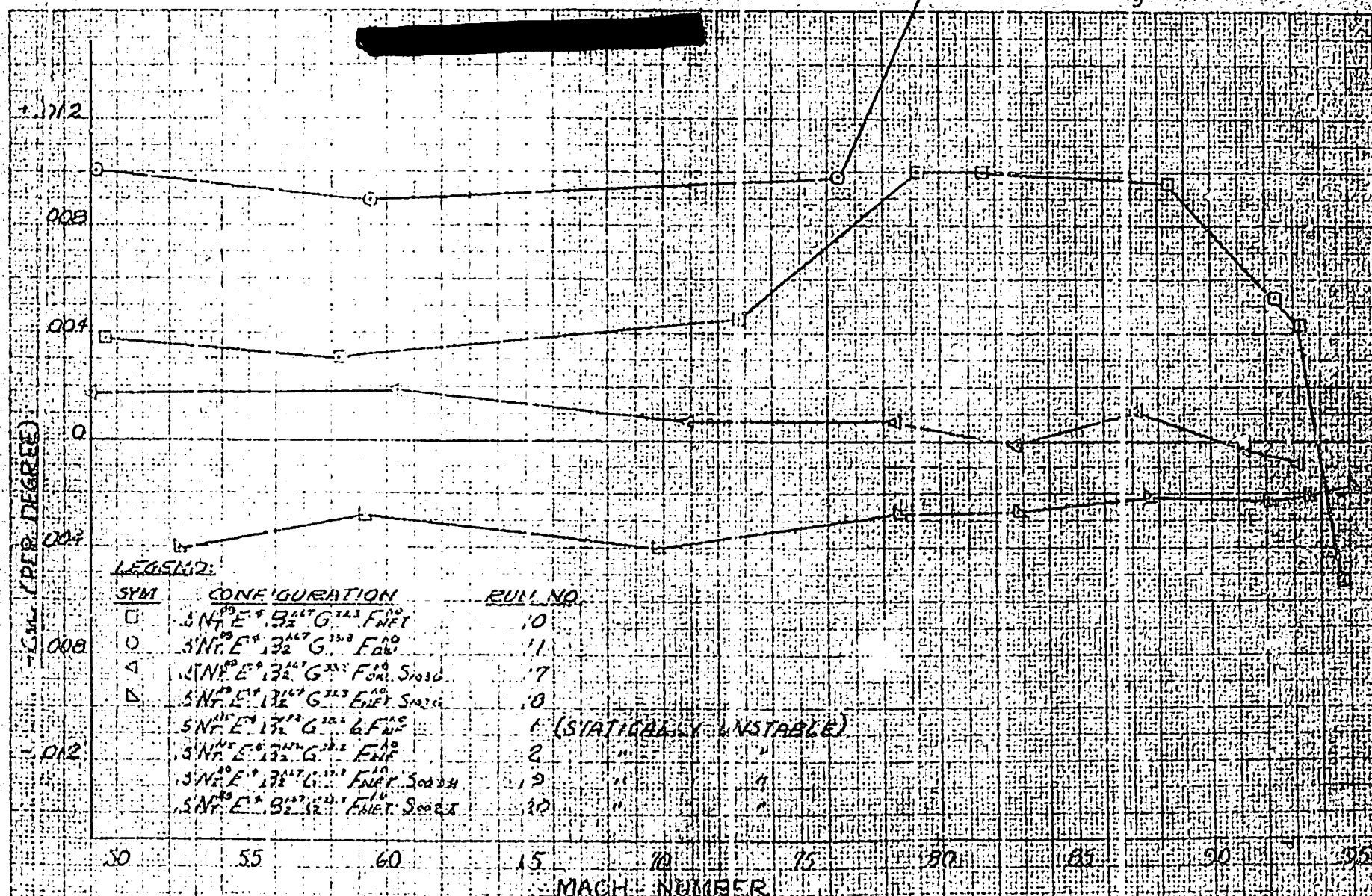

FIGURE 5a, C_{m_α} VS MACH NUMBER (MOD 2)

UNCLASSIFIED

PREP. BY E.J.M. DATE 9-22-54

UNCLASSIFIED

[redacted]

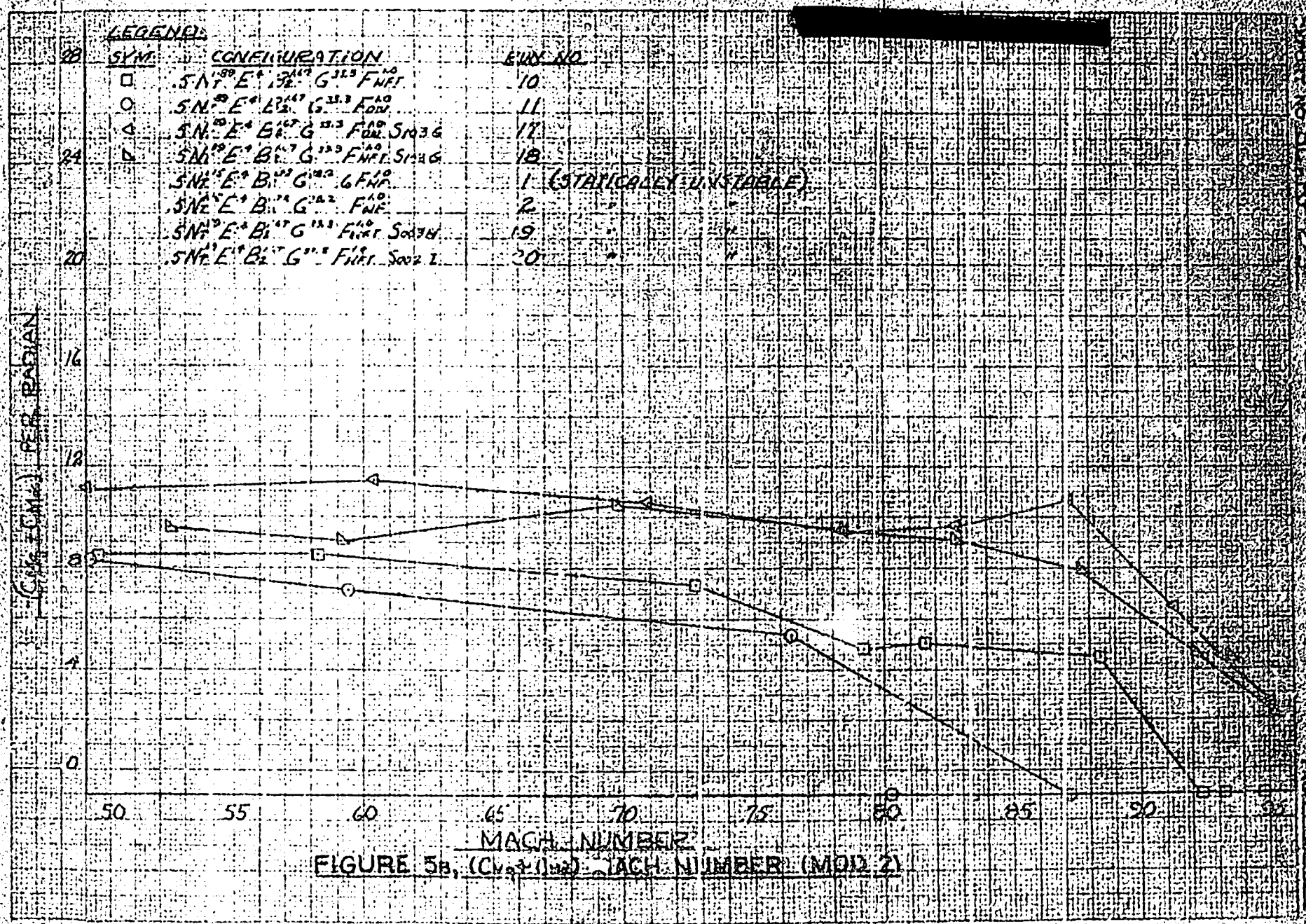

FIGURE 5B, $(C_{m_q}+C_{m_{\dot\alpha}})$ VS MACH NUMBER (MOD 2)

UNCLASSIFIED

UNCLASSIFIED

[redacted]

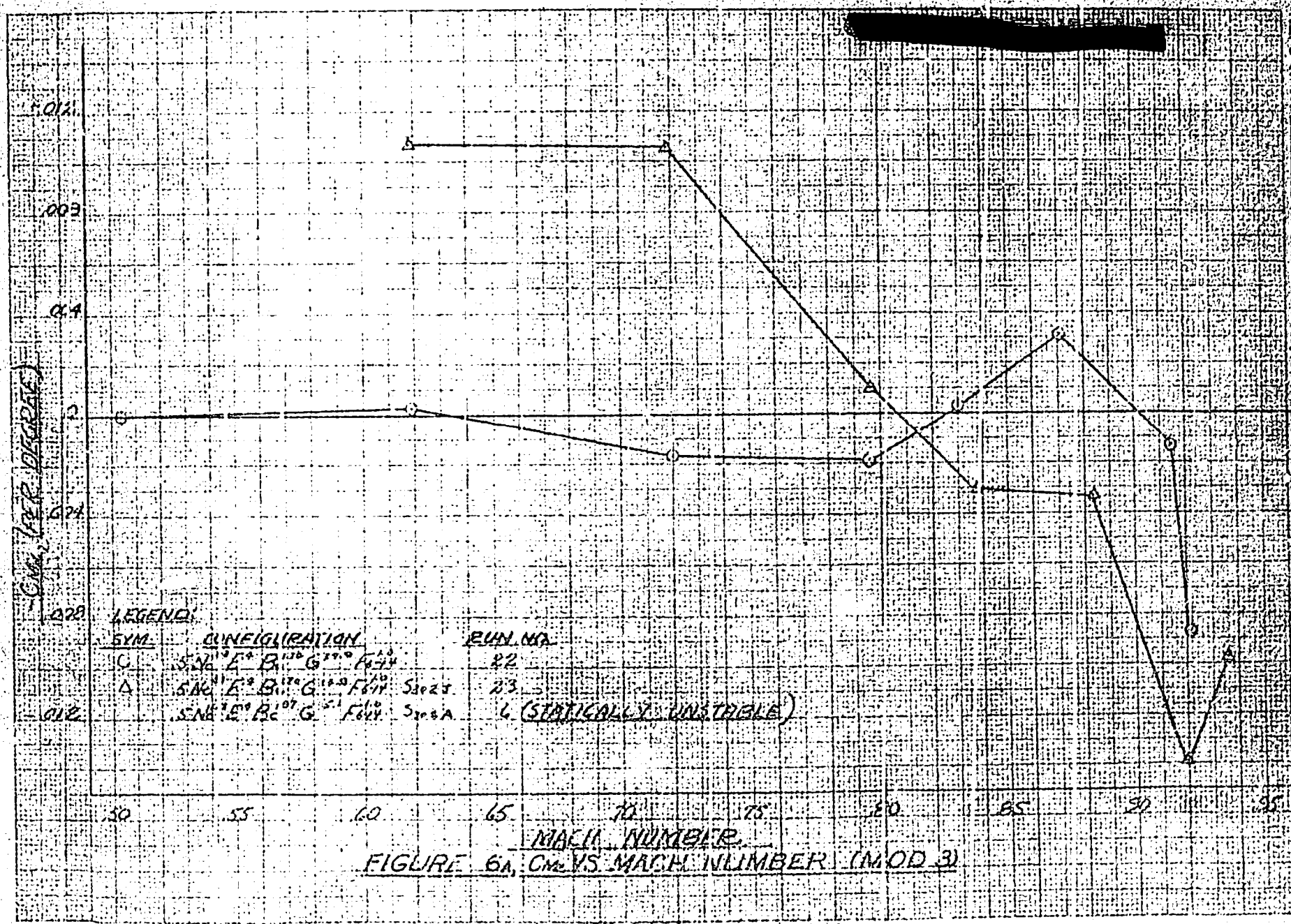

FIGURE 6A, C_{M_α} VS MACH NUMBER (MOD 3)

UNCLASSIFIED

PREP. BY E.N.M. DATE 11-1-76

UNCLASSIFIED

[redacted]

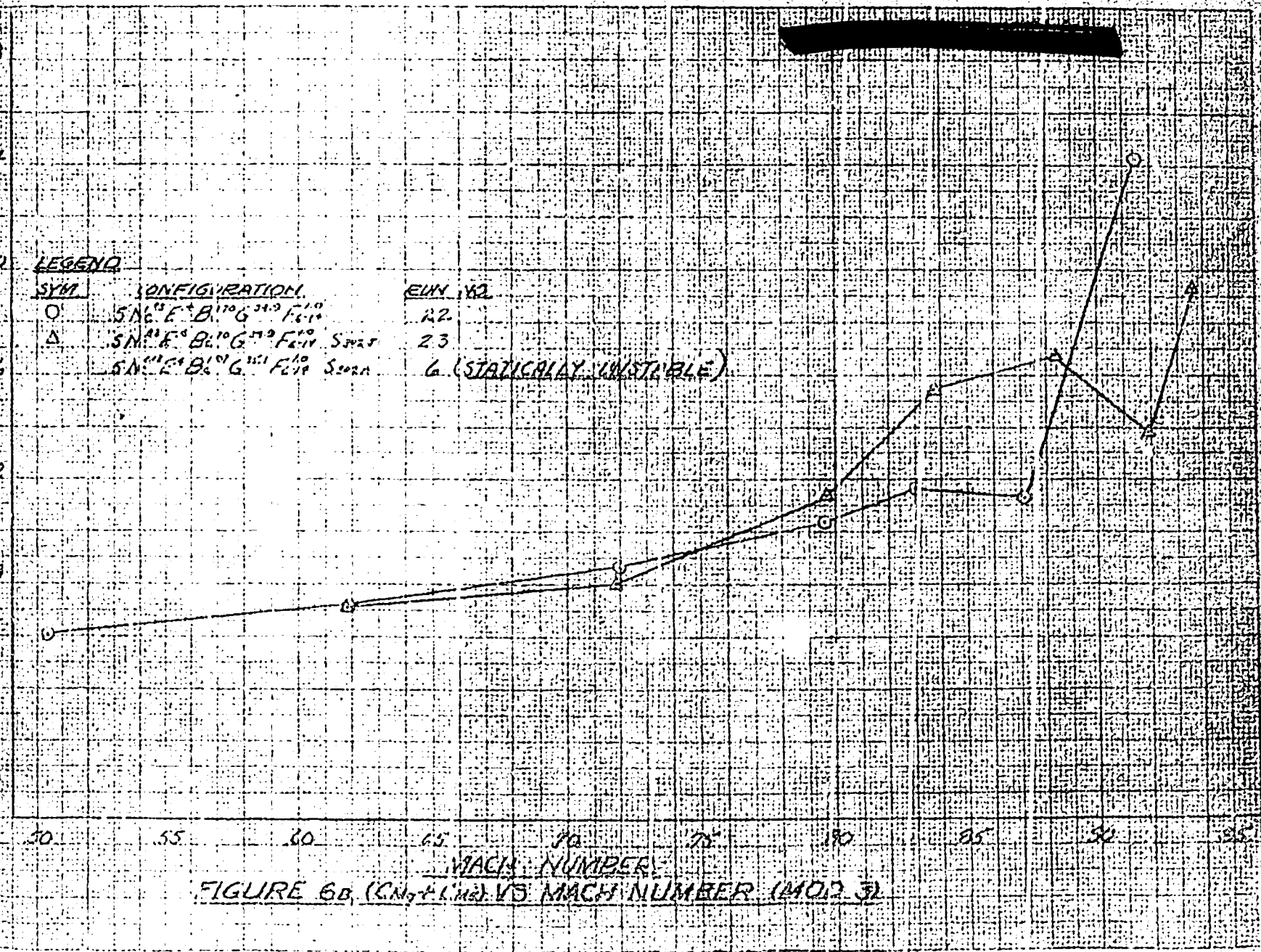

FIGURE 6B ($C_{N_\alpha} + C_{N_{\dot\alpha}}$) VS MACH NUMBER (MOD 3)

UNCLASSIFIED

REPORT NO. SCARF 2-3
SANDIA CORPORATION
ALBUQUERQUE, NEW MEXICO
PAGE 001500

UNCLASSIFIED

[redacted]

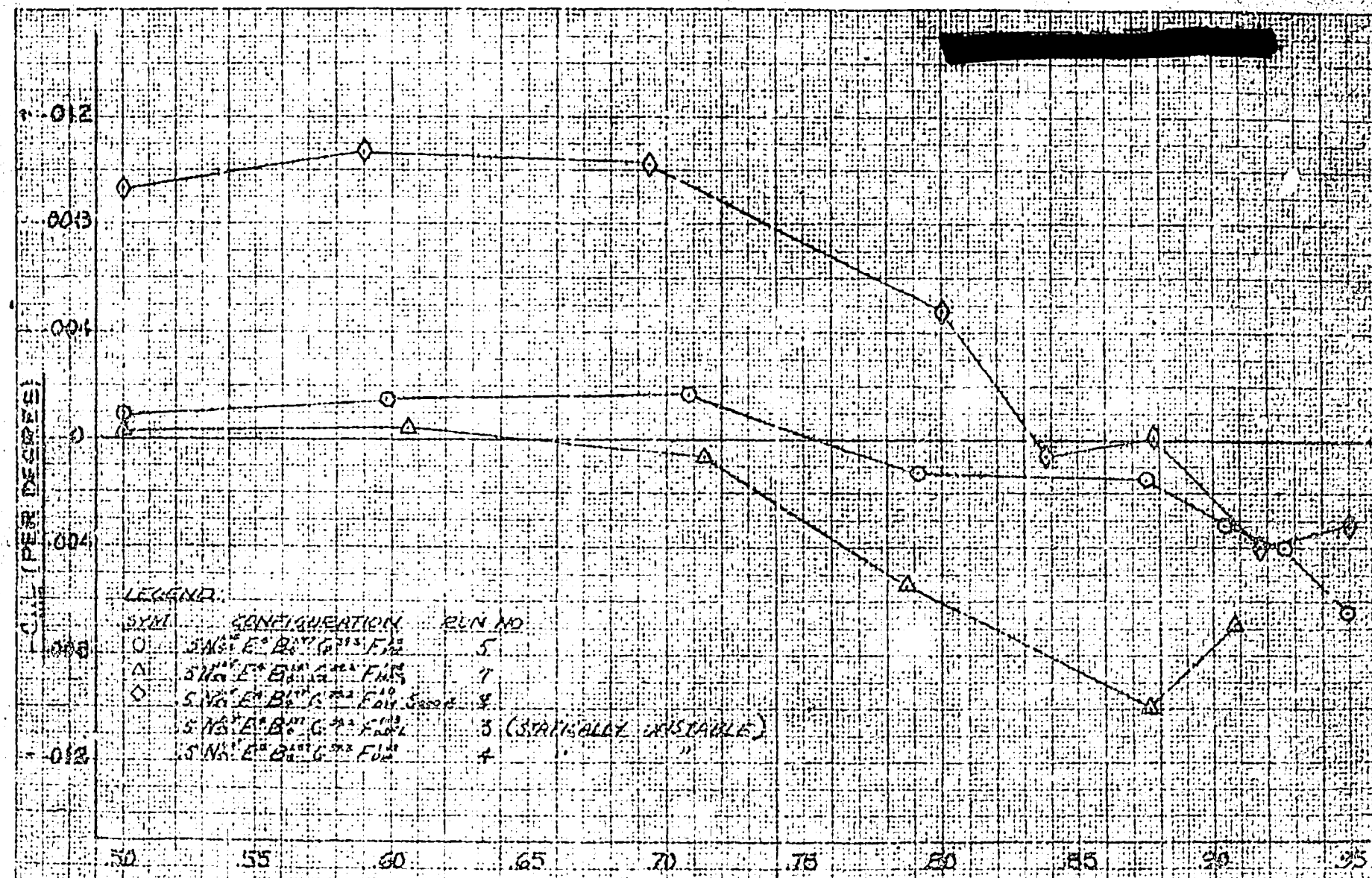

FIGURE 7A. C_{M_α} VS MACH NUMBER (MOD A)

UNCLASSIFIED

PREP. BY R.L.B. DATE 11 SEPT. '54

UNCLASSIFIED

[redacted]

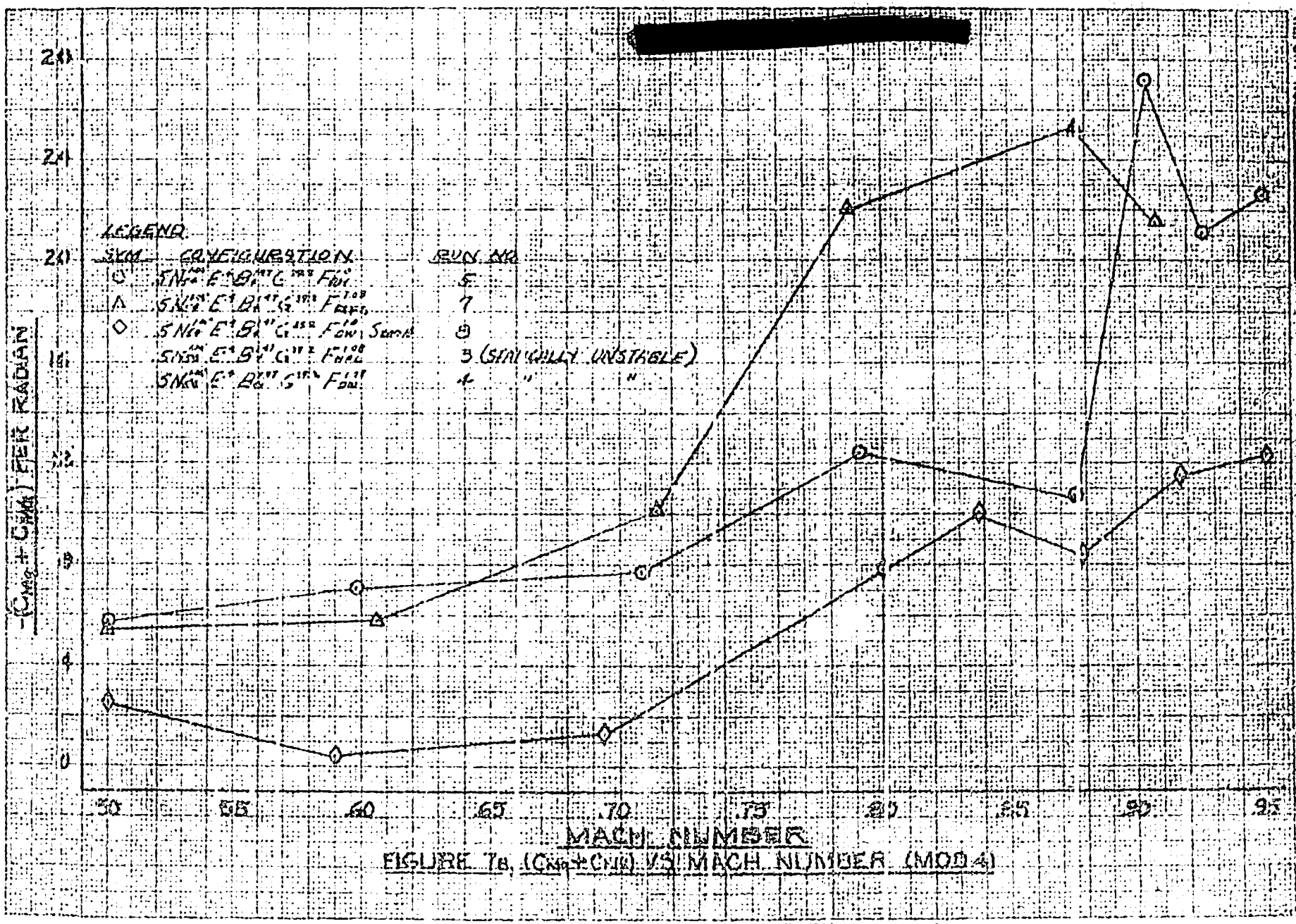

FIGURE 7B, $(C_{N_q} + C_{N_\alpha})$ VS MACH NUMBER (MOD 4)

UNCLASSIFIED

UNCLASSIFIED

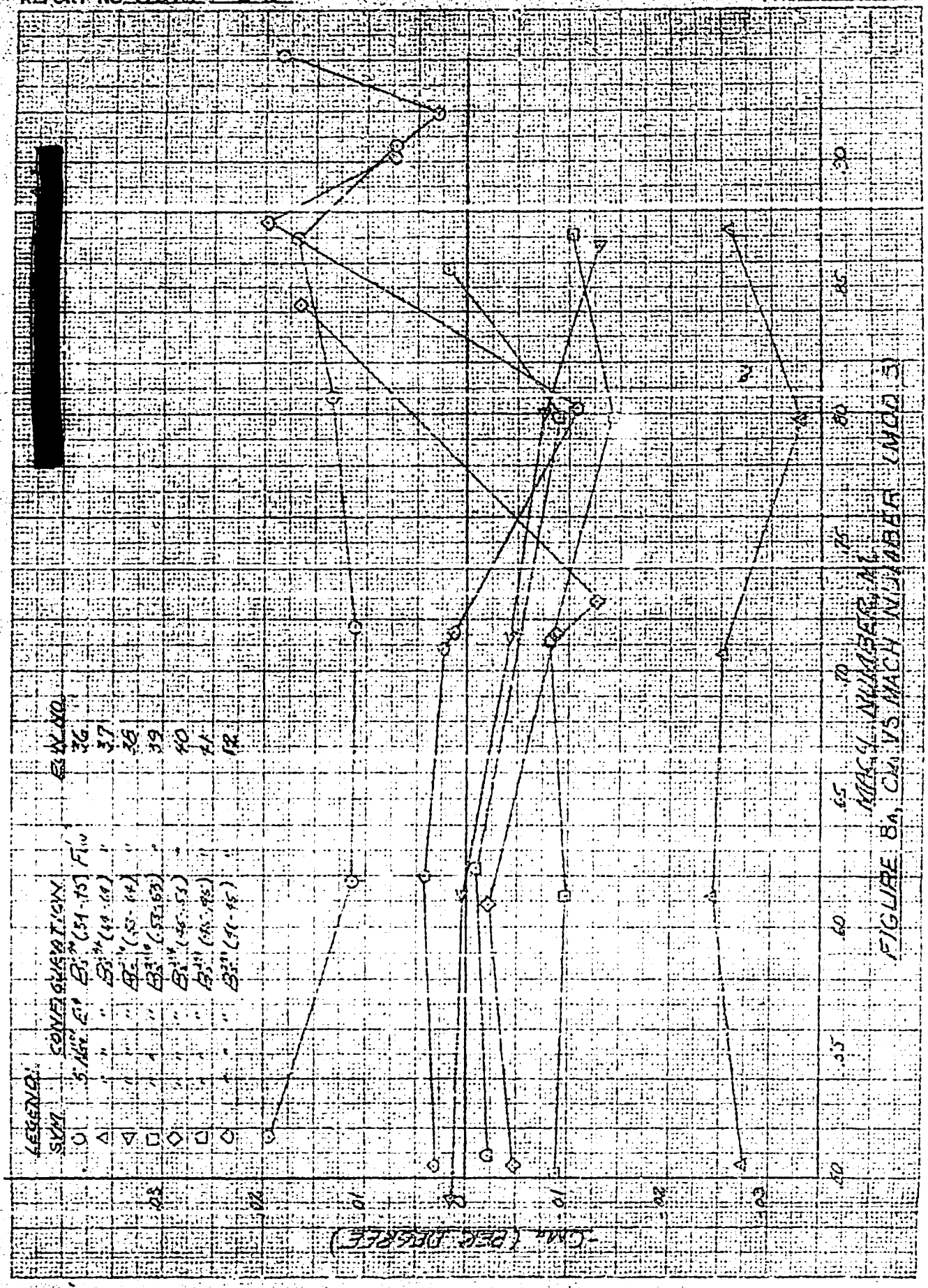

FIGURE 8A, C_{M_α} VS MACH NUMBER (MOD 3)

UNCLASSIFIED

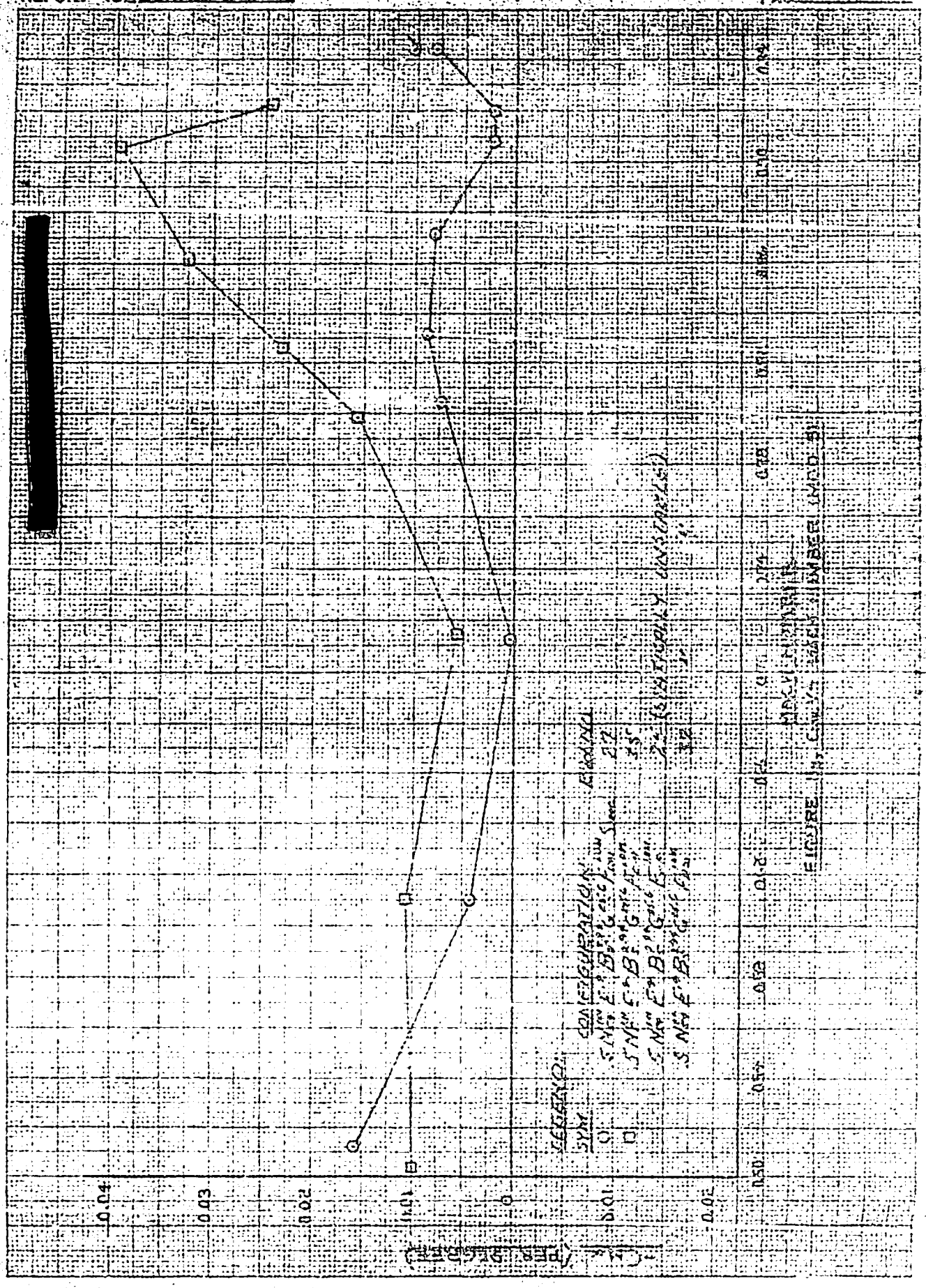

FIGURE 11, CONFIGURATION NUMBER (MOD 5)

PREP. BY E.J.M. DATE 11/14/58

UNCLASSIFIED

UNCLASSIFIED

SANDIA CORPORATION
ALBUQUERQUE, NEW MEXICO

REPORT NO. SCARE 2-3 PAGE

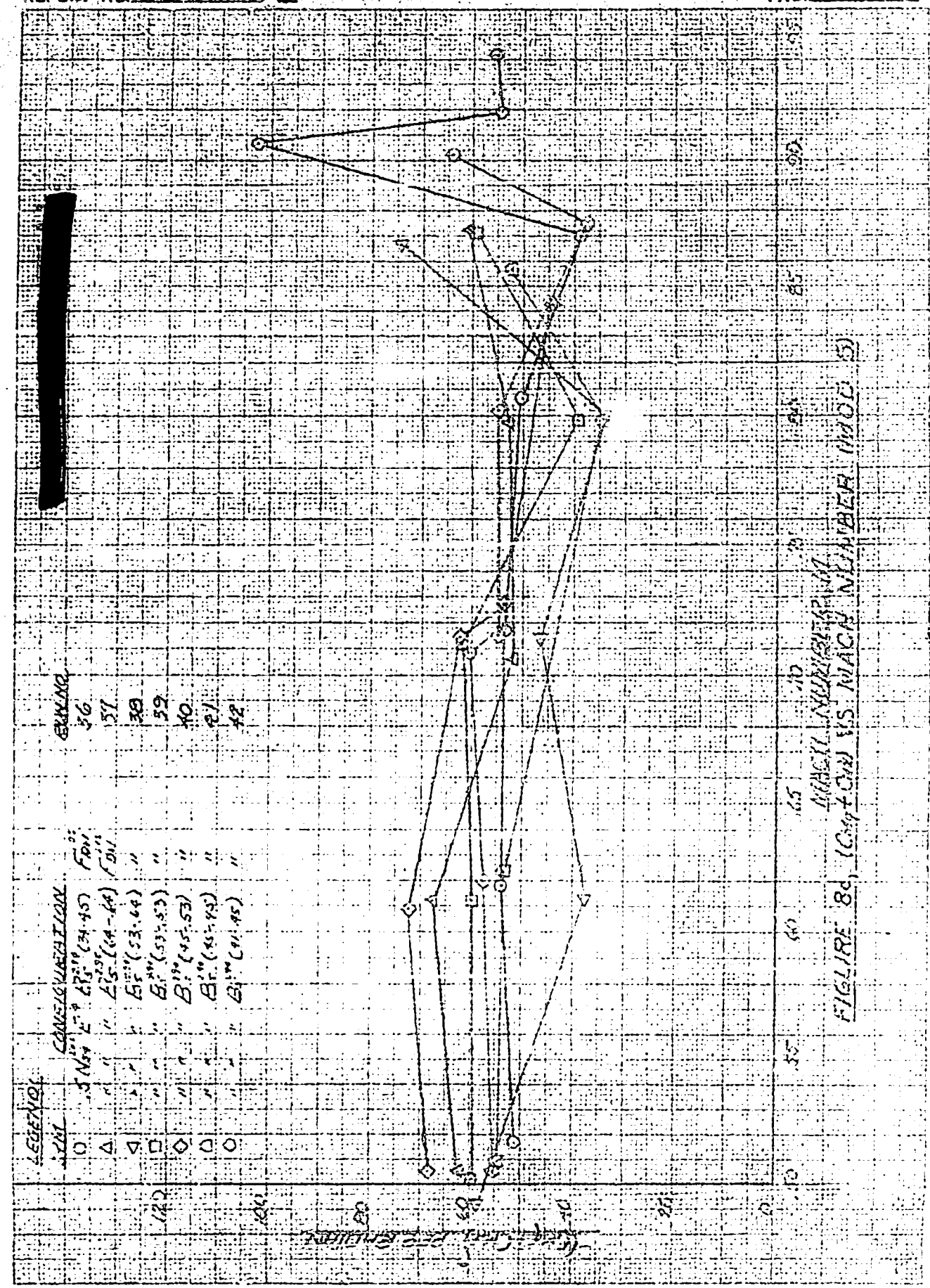

FIGURE 8d (Cont'd) VS MACH NUMBER (MOD 5)

PREP. BY E.J.M. DATE

UNCLASSIFIED

UNCLASSIFIED

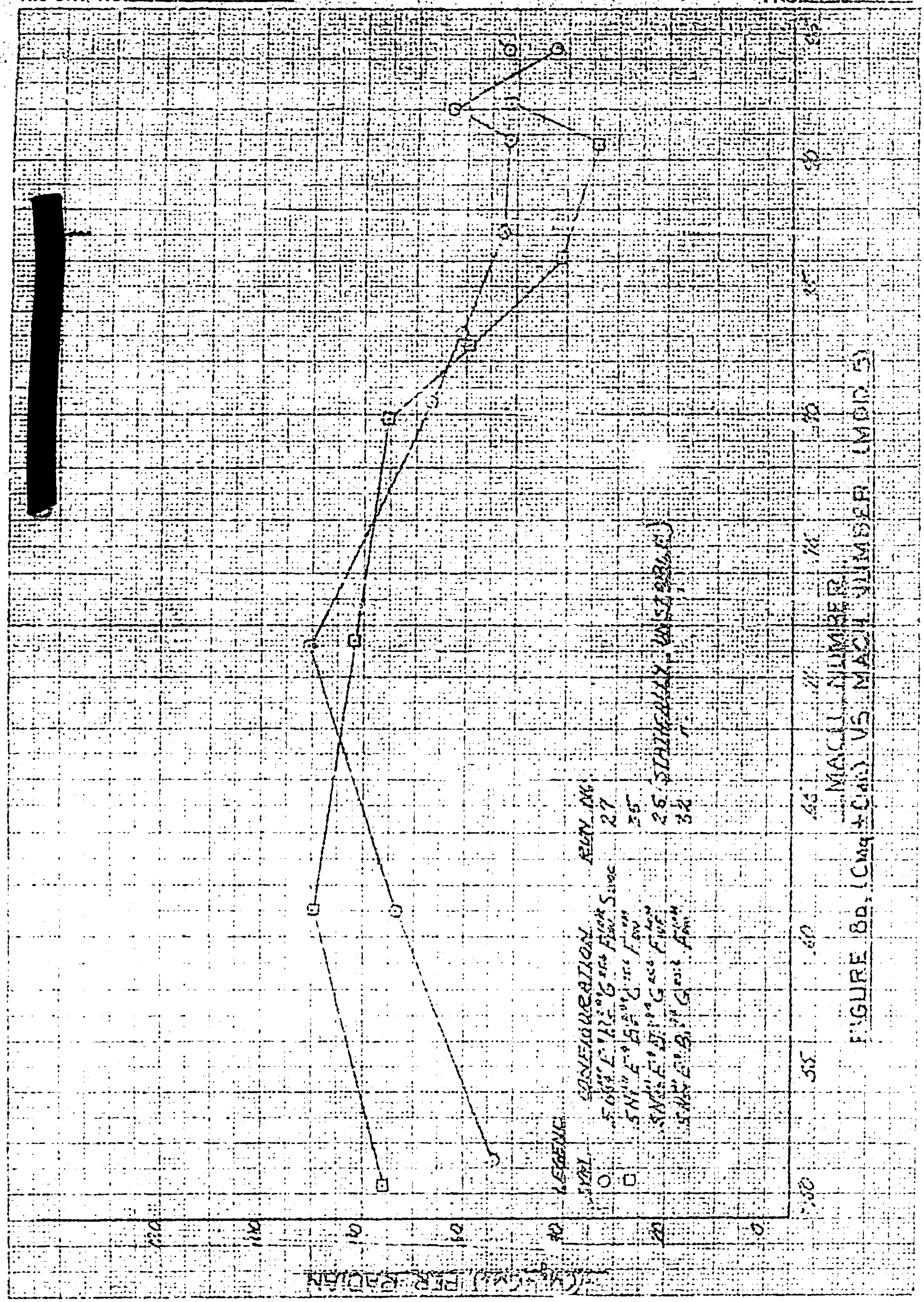

[redacted]

FIGURE 8a. (C_{mq} + $C_{m\dot{\alpha}}$) VS MACH NUMBER (MOD 5)

UNCLASSIFIED

UNCLASSIFIED

[redacted]

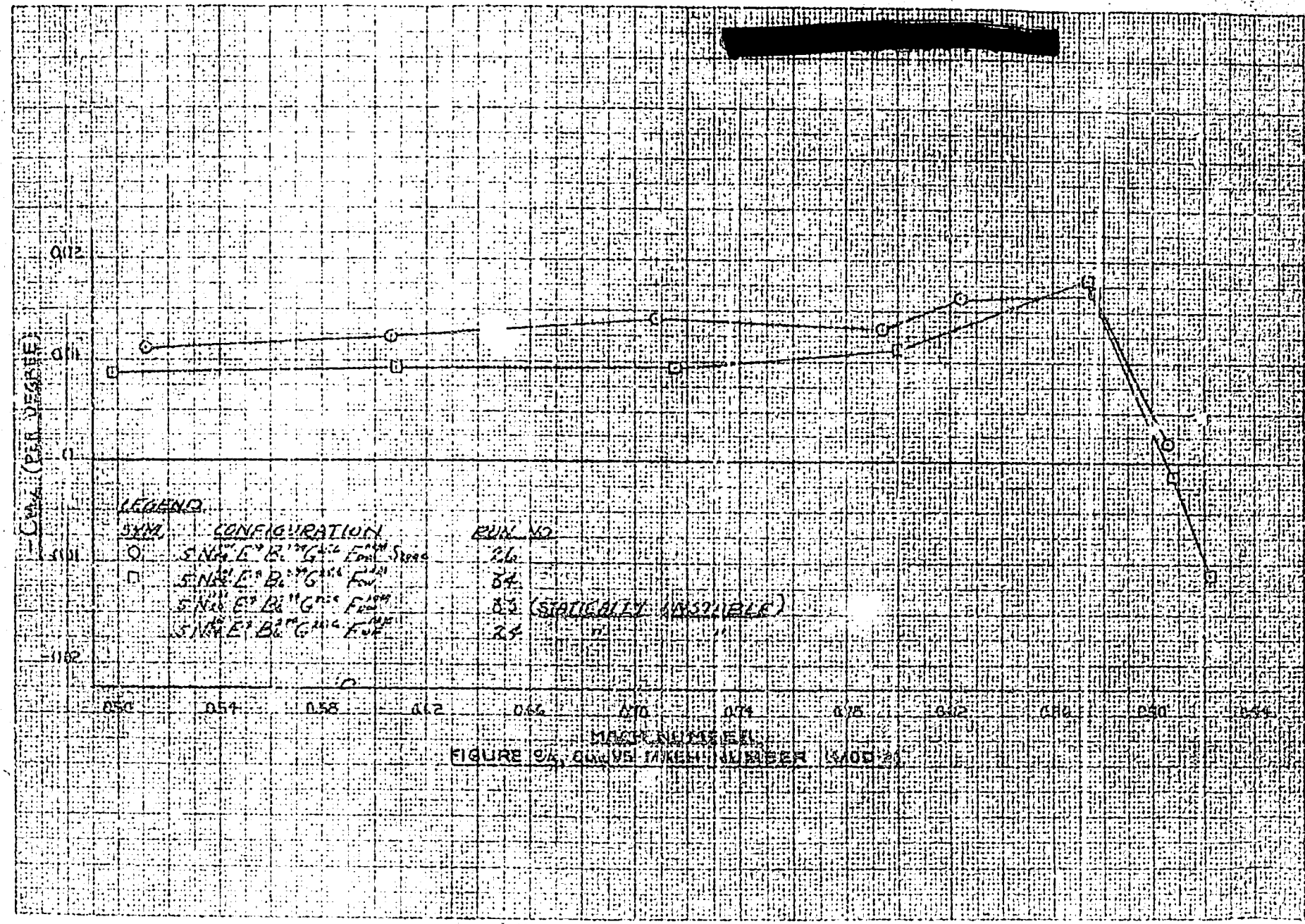

FIGURE 94, CURVES MACH NUMBER MOD-21

UNCLASSIFIED

PREP. BY
DATE

UNCLASSIFIED

[redacted]

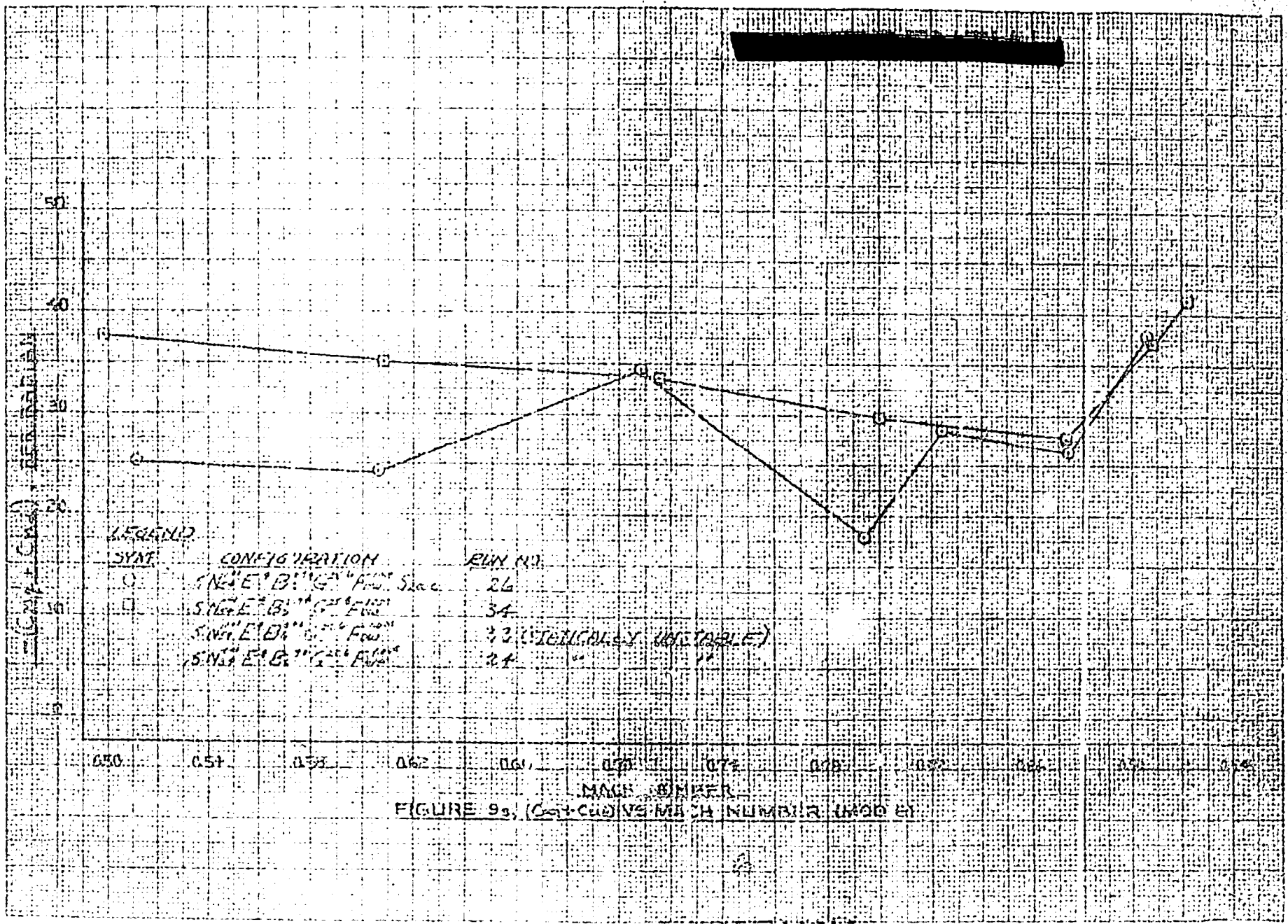

FIGURE 9a, (Cm+Cue) VS MACH NUMBER (MOD 6)

UNCLASSIFIED

PREP. BY E.J.K. DATE

UNCLASSIFIED

[redacted]

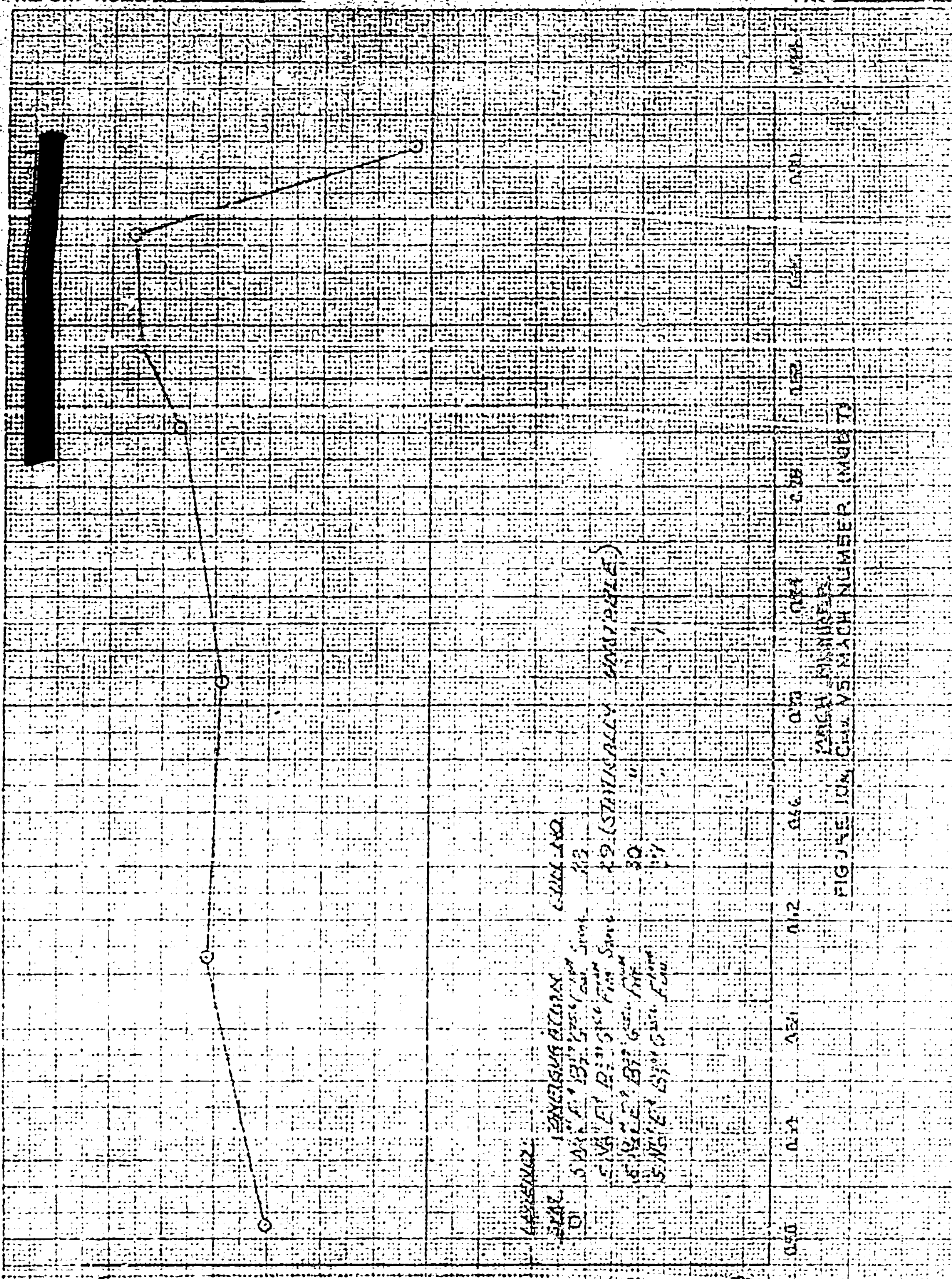

FIGURE 10N, C_M VS MACH NUMBER (MACH T)

PREP. BY E.J.M DATE

SANDIA CORPORATION
ALBUQUERQUE, NEW MEXICO
REPORT NO. SCARF 2-3
PAGE

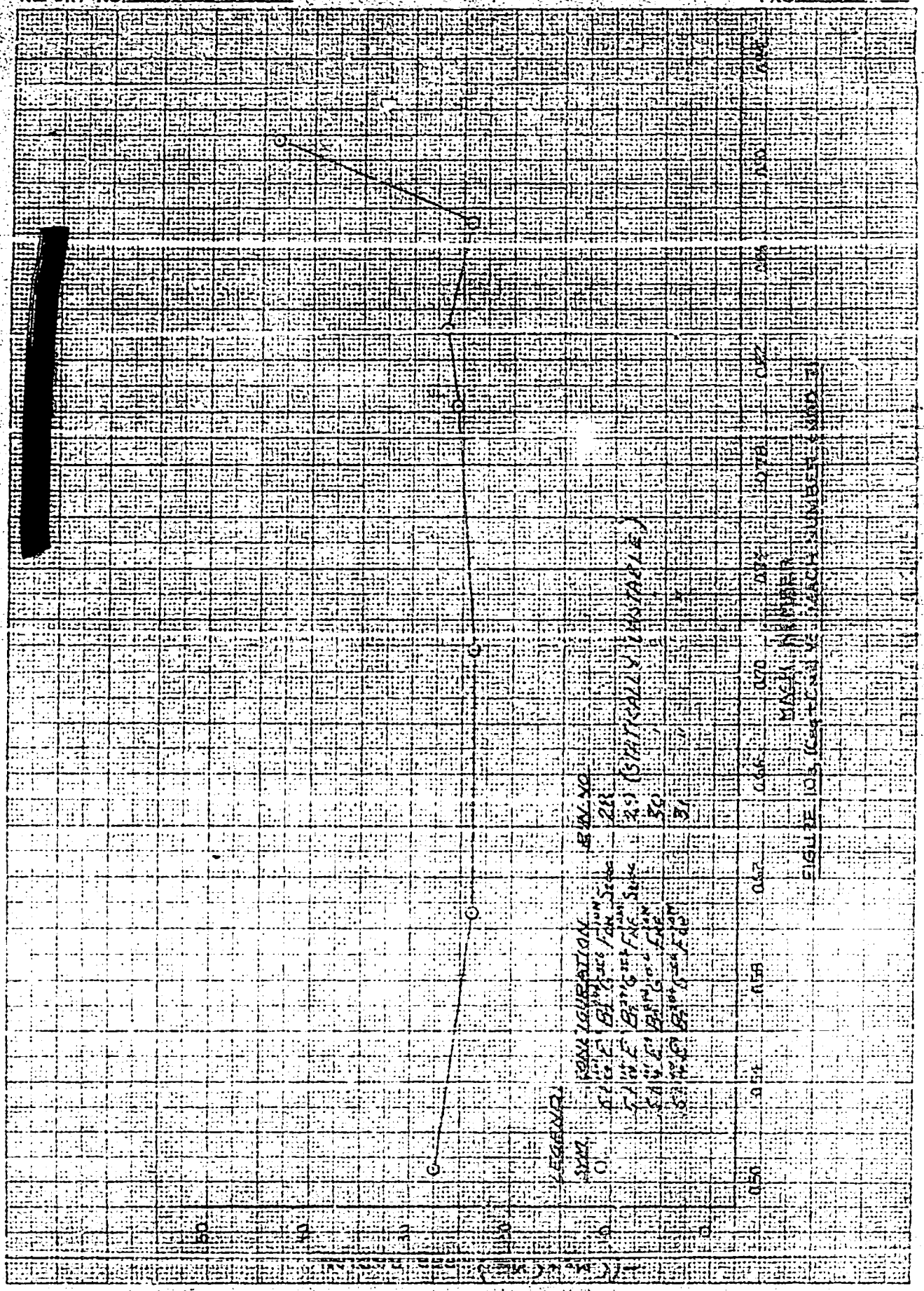

UNCLASSIFIED

SANDIA CORPORATION
ALBUQUERQUE, NEW MEXICO
SCARF 2-3

UNCLASSIFIED

[redacted]

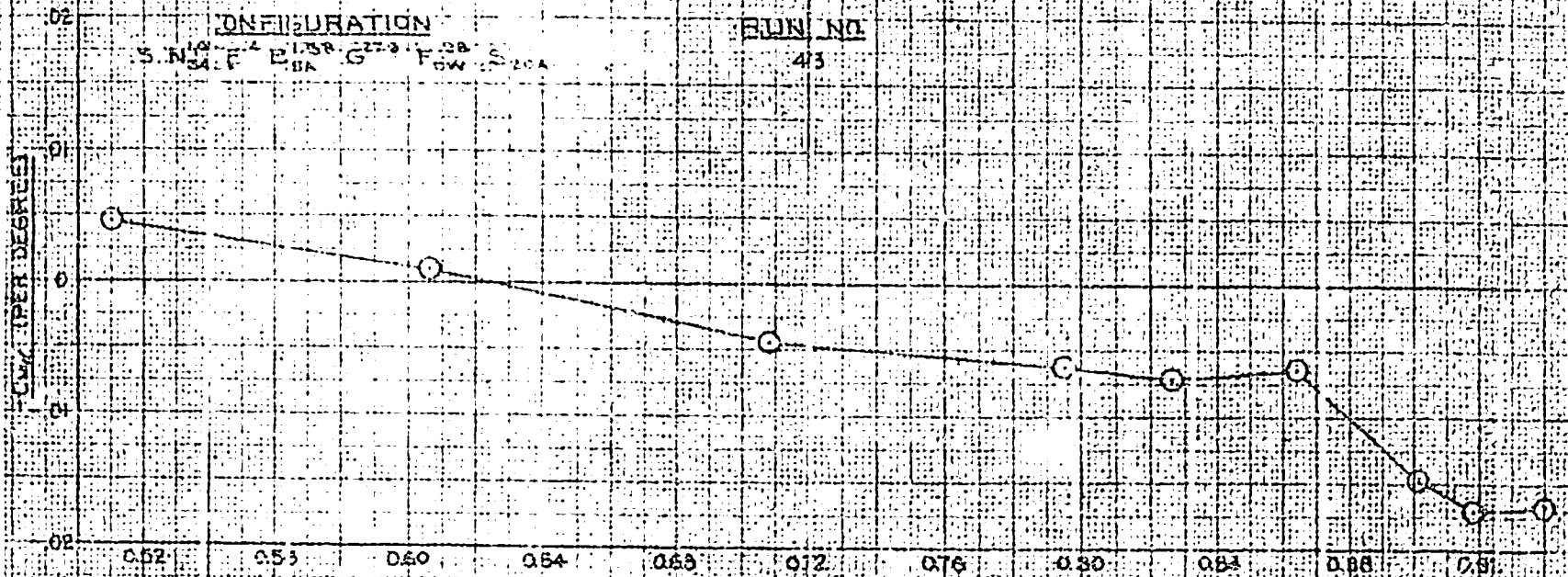

FIGURE 11A, C_{m_α} VS MACH NUMBER (MOD. 6)

UNCLASSIFIED

PREP. BY

UNCLASSIFIED

[redacted]

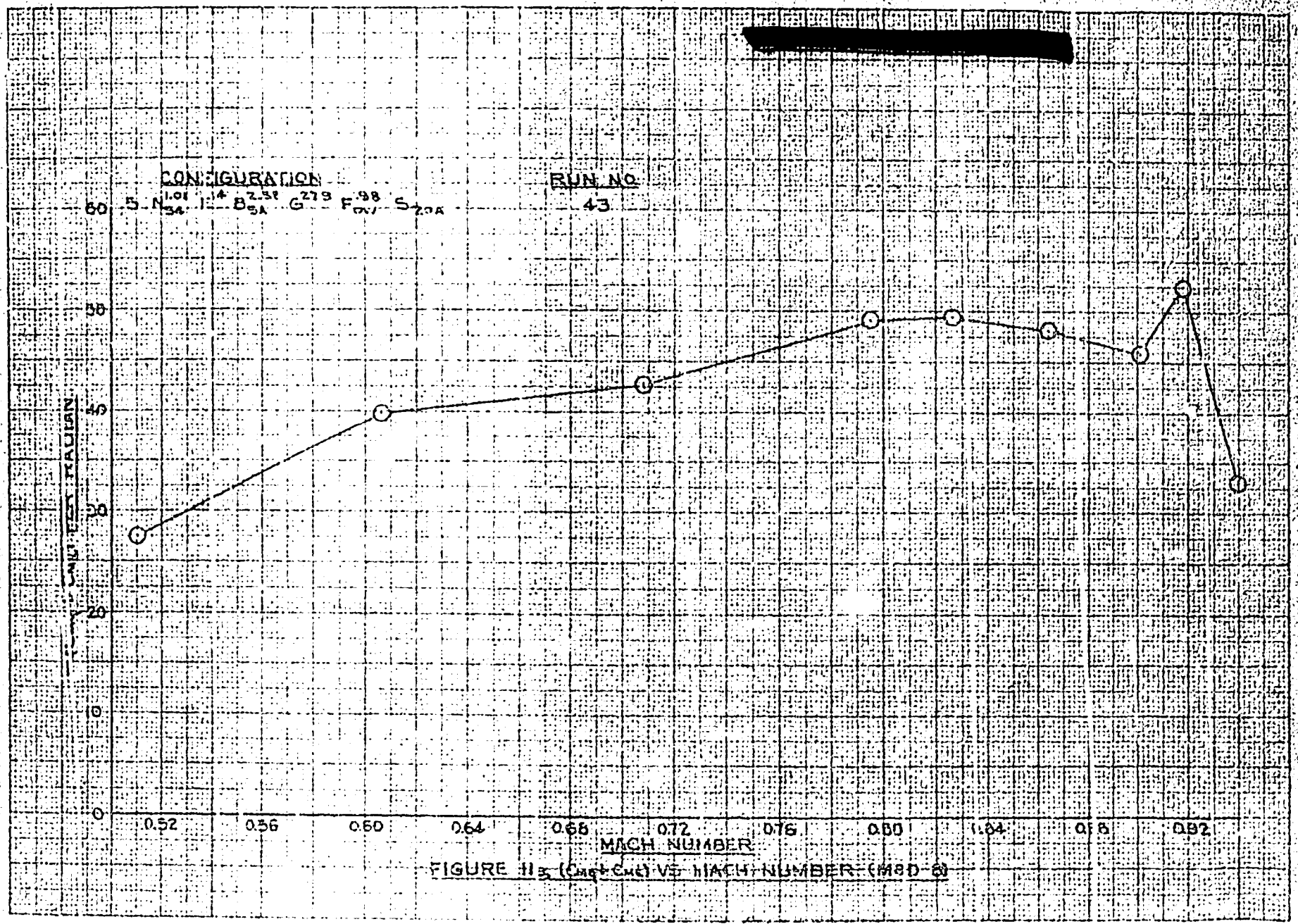

FIGURE 113 ($C_{mq}+C_{m\dot{\alpha}}$) VS MACH NUMBER (M8D-6)

UNCLASSIFIED

UNCLASSIFIED

[redacted]

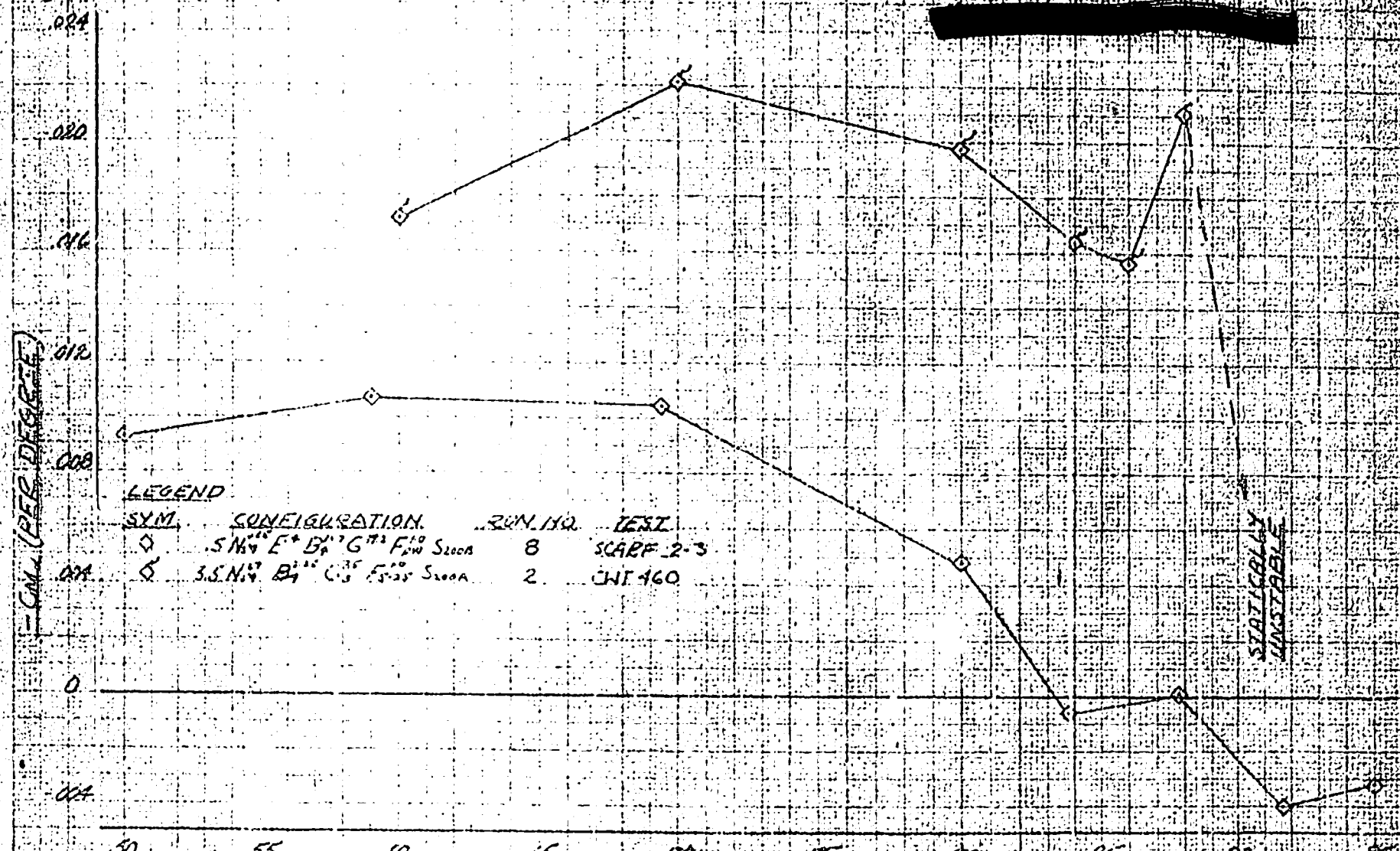

FIGURE 12A. COMPARISON OF THE STATIC STABILITY COEFFICIENTS OBTAINED IN CWT AND SCARF 2 ON MODELS OF THE SHORT 7 MOD. 4

UNCLASSIFIED

PREP. BY [illegible] DATE [illegible]

UNCLASSIFIED

[redacted]

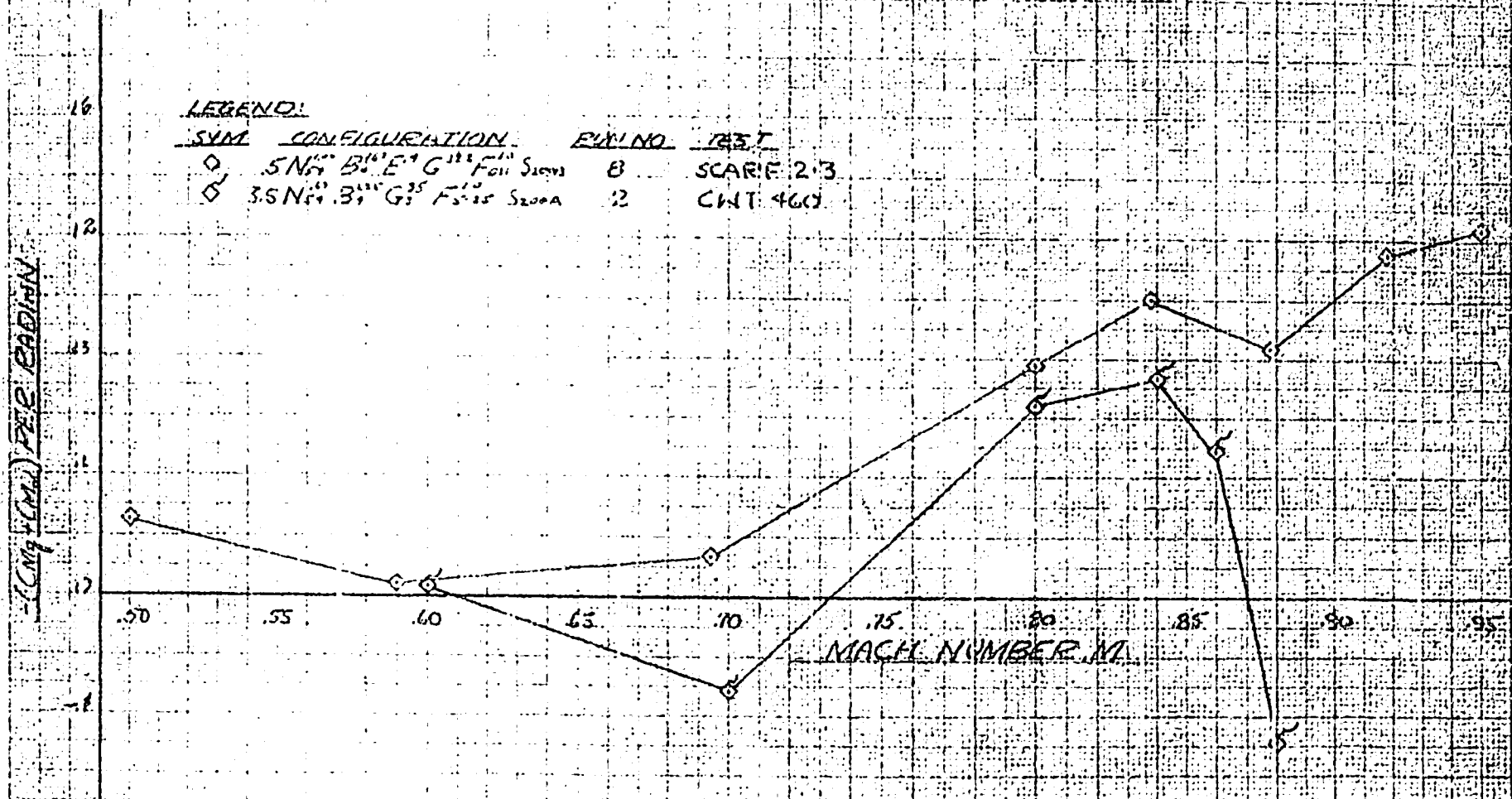

FIGURE 12B, COMPARISON OF THE DYNAMIC STABILITY COEFFICIENTS OBTAINED IN CWT AND SCARF 2 ON MODELS OF THE SHORT 7 MOD 1

UNCLASSIFIED

10 X 10 TO THE CM. 359-14

UNCLASSIFIED

[redacted]

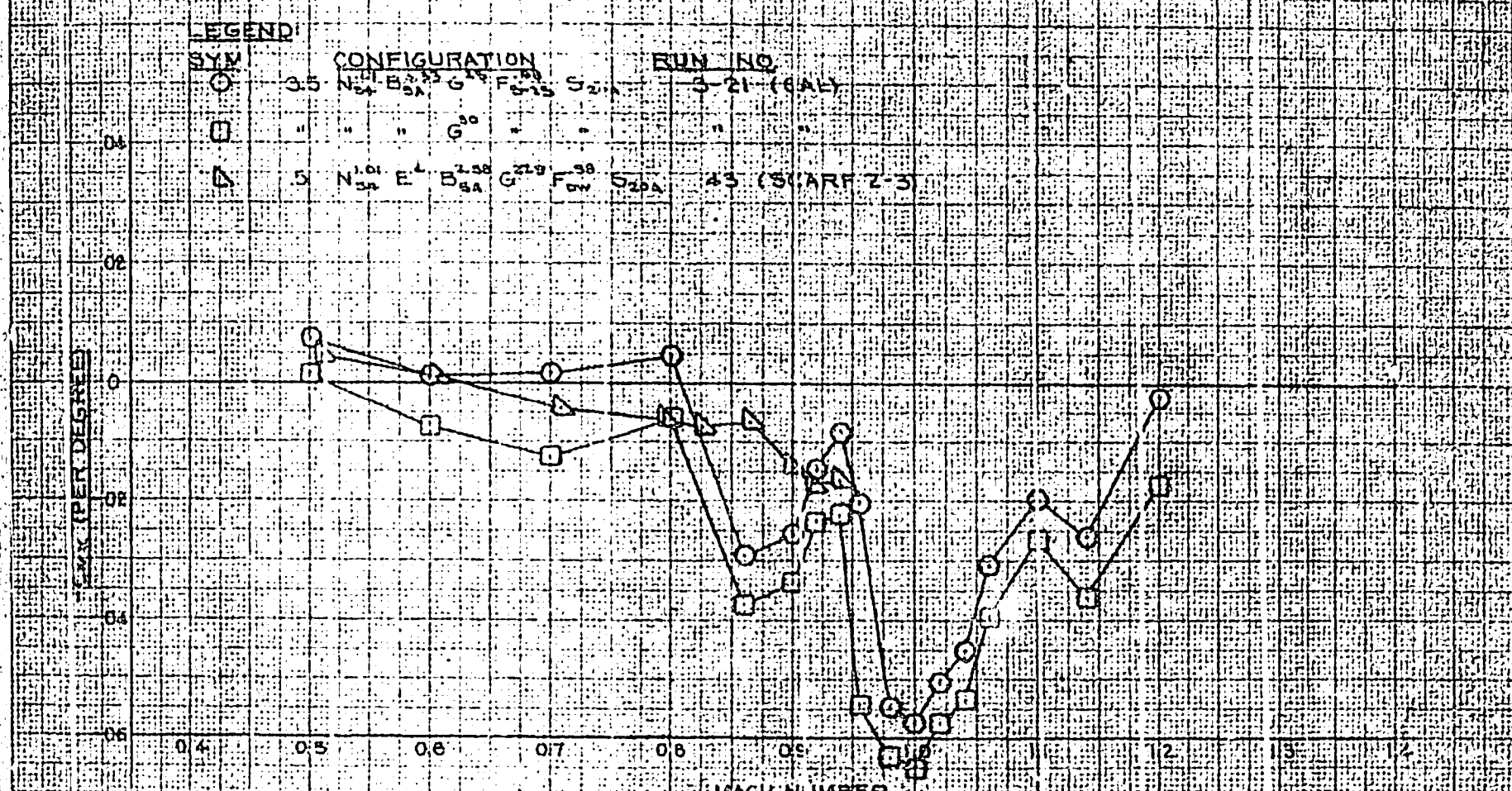

FIGURE 13. COMPARISON OF C_{MX} OBTAINED IN CAL AND SCARF II ON MODELS OF THE SHORT T MOD

UNCLASSIFIED

SANDIA CORPORATION
ALBUQUERQUE, NEW MEXICO
REPORT NO. 004594

PREP. BY _____ DATE _____

UNCLASSIFIED

[redacted]

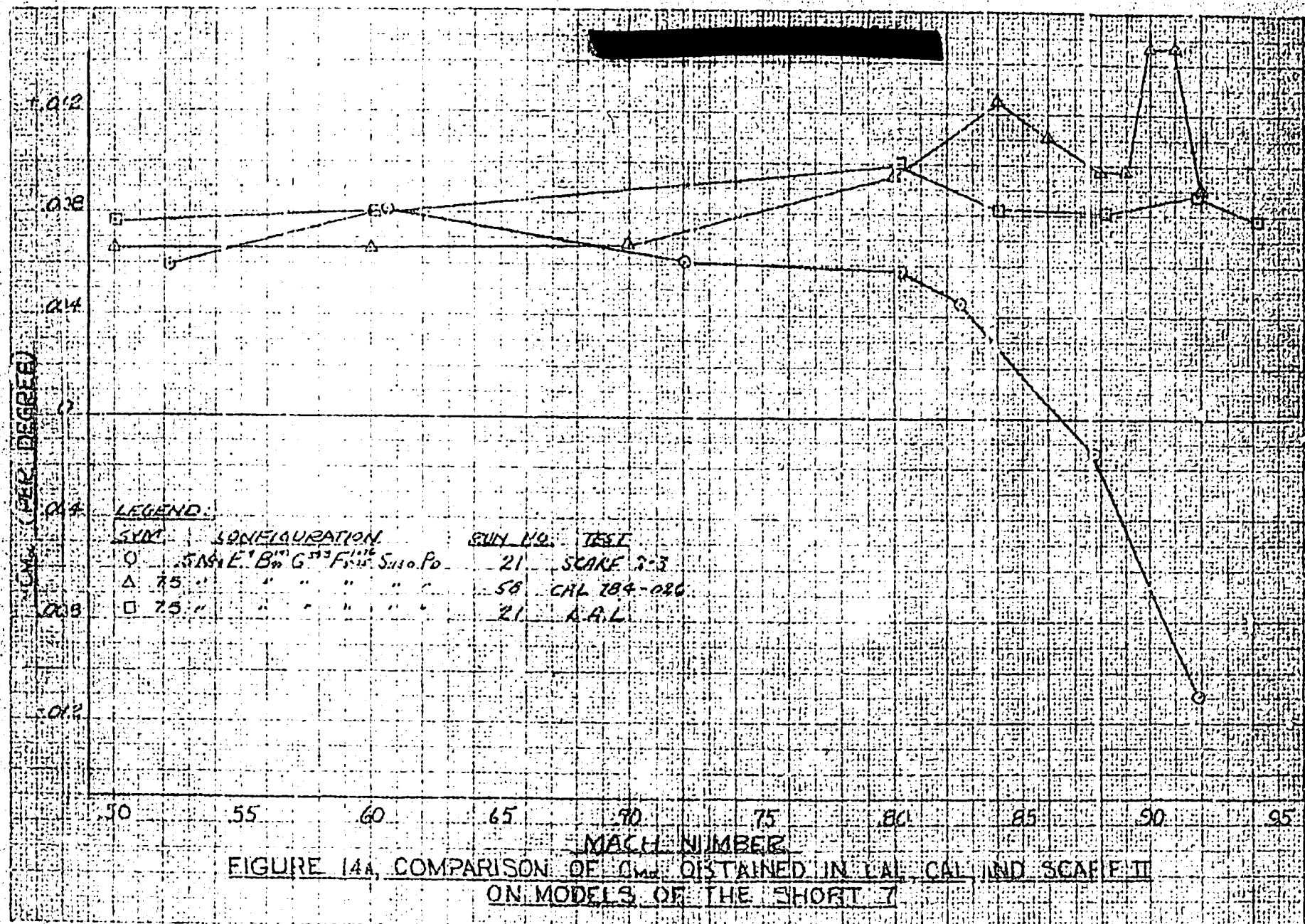

FIGURE 14A, COMPARISON OF C_{m_α} OBTAINED IN LAL, CAL AND SCAFF II ON MODELS OF THE SHORT 7

UNCLASSIFIED

REPORT NO.
SANDIA CORPORATION
ALBUQUERQUE, NEW MEXICO
PAGE
PREP. BY
DATE

SANDIA CORPORATION
ALBUQUERQUE, NEW MEXICO
REPORT NO.
PAGE

UNCLASSIFIED

[redacted]

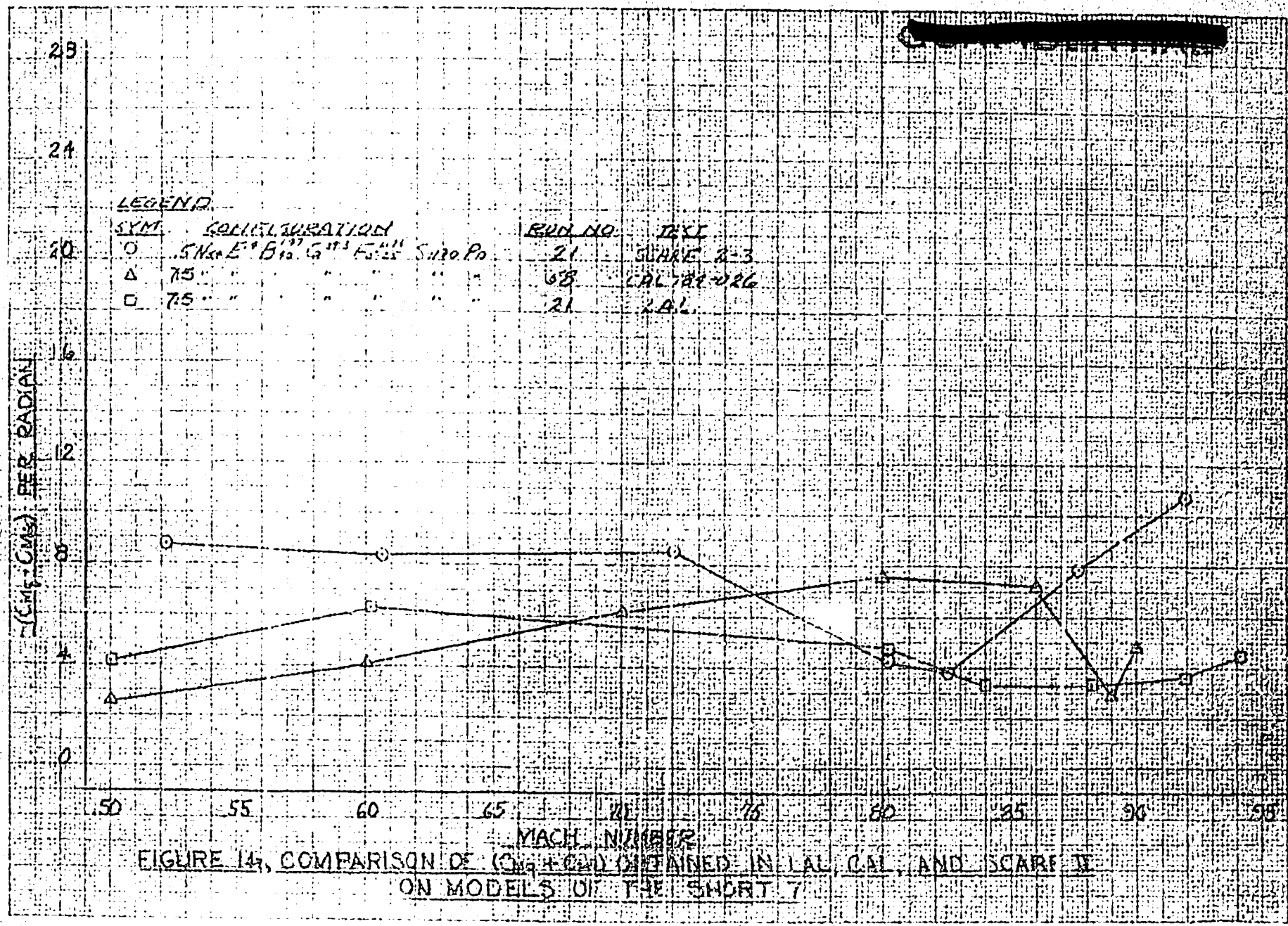

FIGURE 14, COMPARISON OF (CMq + CMq) OBTAINED IN LAL, CAL, AND SCARE II ON MODELS OF THE SHORT 7

UNCLASSIFIED

PREP. BY EJM DATE 9-27-54

REPORT NO. CWT 460
SANDIA CORPORATION
ALBUQUERQUE, NEW MEXICO
PAGE 11

UNCLASSIFIED

[redacted]

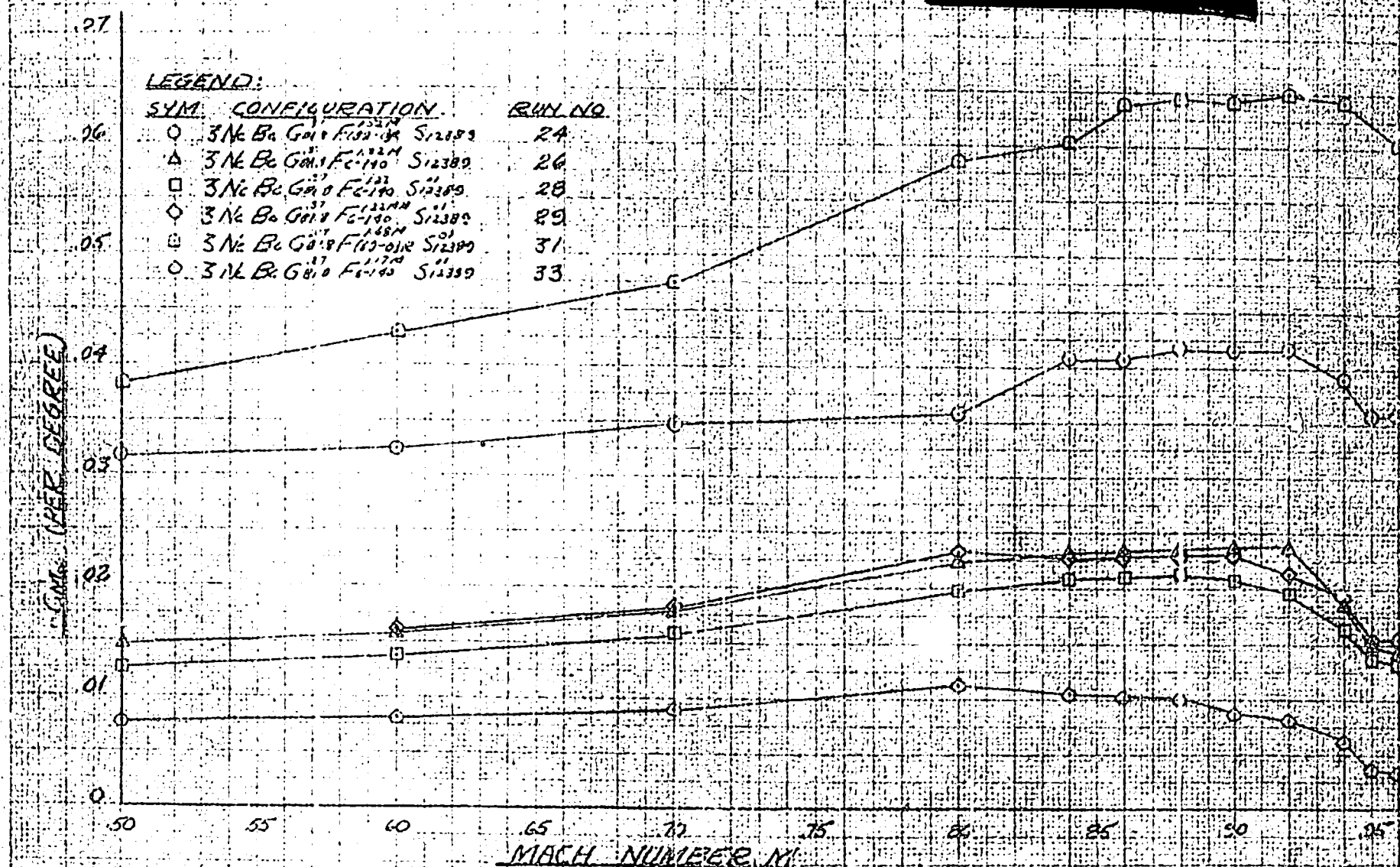

FIGURE 15a. STATIC STABILITY CHARACTERISTICS OF THE TX-14 (CARRIE) WITH DIFFERENT FIN CONFIGURATIONS

UNCLASSIFIED

001597

UNCLASSIFIED

[redacted]

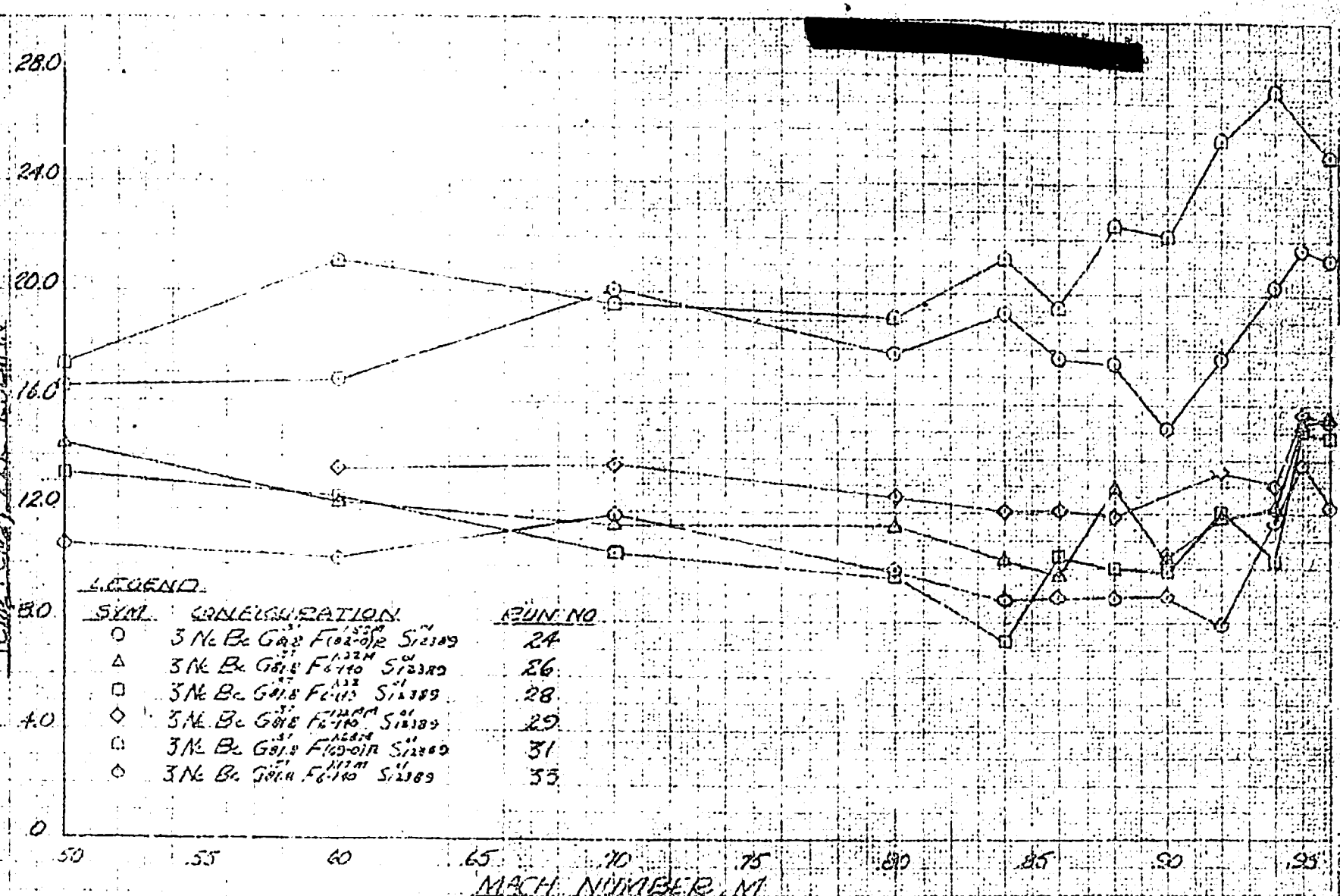

FIGURE 15. DYNAMIC STABILITY CHARACTERISTICS OF THE TX-14 (CARRIE) WITH DIFFERENT FIN CONFIGURATIONS

UNCLASSIFIED

UNCLASSIFIED

[redacted]

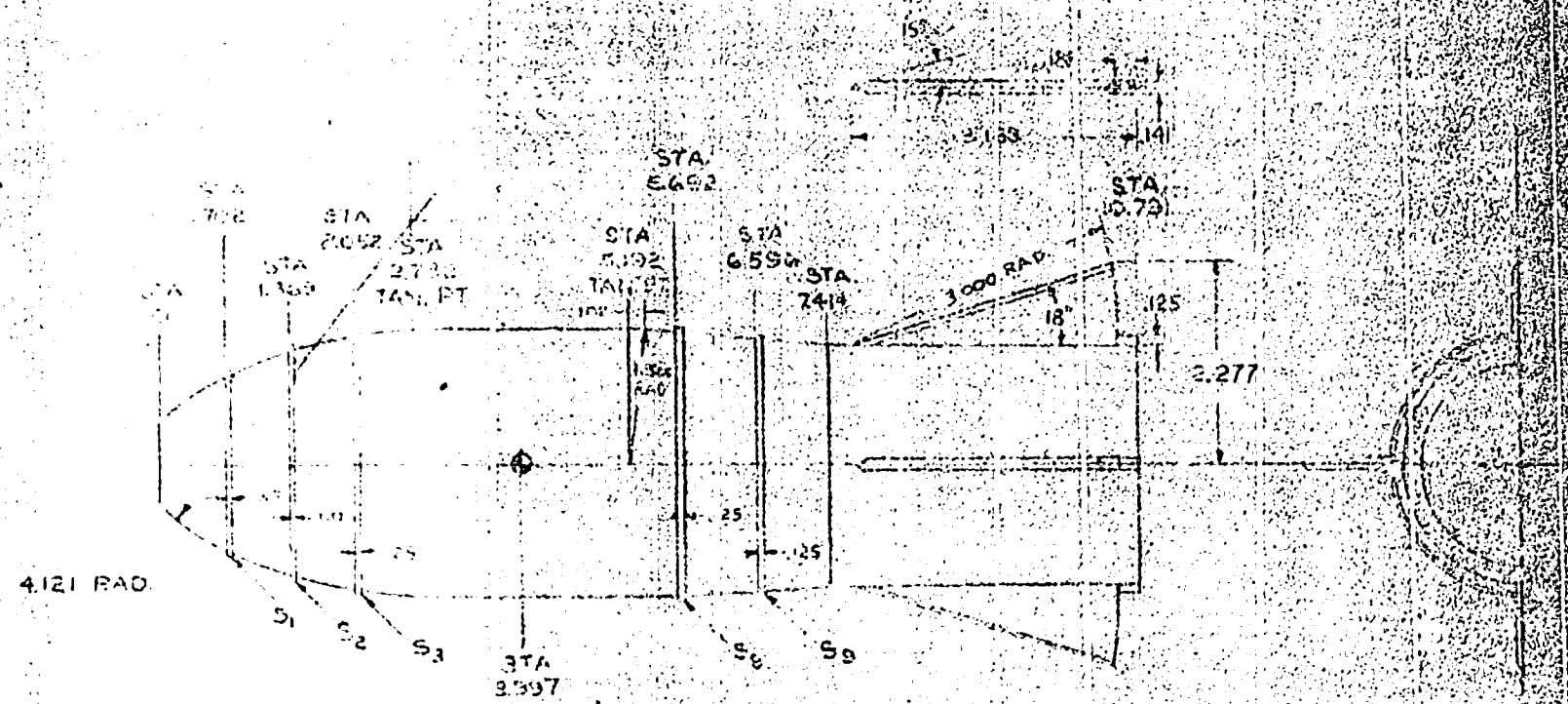

ALL SPOILER BANDS PROJECT
0.037 ABOVE THE SURFACE OF
THE MODEL AT THE LEADING EDGES.

MODEL ORDINATES	
STA	DIA.
0	.328
2.732	3.000
5.192	3.000
7.414	2.100
10.791	2.100

UNCLASSIFIED

FIGURE 18

RETRACTABLE FIN TX-14 (CARRIE) SHAPE

3 No. Bc Fig. [illegible] S12565